

Guaranteeing Privacy in Hybrid Quantum Learning through Theoretical Mechanisms

Hoang M. Ngo¹ Tre' R. Jeter^{1,2} Incheol Shin³ Wanli Xing⁴ Tamer Kahveci¹ My T. Thai¹

Abstract

Quantum Machine Learning (QML) is becoming increasingly prevalent due to its potential to enhance classical machine learning (ML) tasks, such as classification. Although quantum noise is often viewed as a major challenge in quantum computing, it also offers a unique opportunity to enhance privacy. In particular, intrinsic quantum noise provides a natural stochastic resource that, when rigorously analyzed within the differential privacy (DP) framework and composed with classical mechanisms, can satisfy formal (ϵ, δ) -DP guarantees. This enables a reduction in the required classical perturbation without compromising the privacy budget, potentially improving model utility. However, the integration of classical and quantum noise for privacy preservation remains unexplored. In this work, we propose a hybrid noise-added mechanism, HYPER-Q, that combines classical and quantum noise to protect the privacy of QML models. We provide a comprehensive analysis of its privacy guarantees and establish theoretical bounds on its utility. Empirically, we demonstrate that HYPER-Q outperforms existing classical noise-based mechanisms in terms of adversarial robustness across multiple real-world datasets.

1. Introduction

Quantum Machine Learning (QML) has emerged as a compelling paradigm that integrates the computational advantages of quantum systems with the modeling power of machine learning (ML). A fundamental feature of quantum systems is quantum noise, the inherent randomness and

decoherence that arise due to interactions with the environment. Although quantum noise is typically considered to be a barrier to achieving fault-tolerant quantum computing, it provides an opportunity to serve as a natural and intrinsic source of randomness for privacy-preservation.

In classical ML, Differential Privacy (DP) (Dwork, 2006) has become the standard framework for providing formal privacy guarantees. DP ensures that the output of an algorithm does not change significantly when a single individual's data is added or removed from the input dataset, thereby protecting individual privacy. Beyond its role in privacy preservation, DP has also been extended to certify the robustness of ML models against adversarial attacks (Lecuyer et al., 2019; Cohen et al., 2019). Privacy in DP is typically achieved by injecting carefully calibrated random noise, such as Gaussian or Laplacian, into the learning process (Geng & Viswanath, 2012; Balle & Wang, 2018; Ji & Li, 2024). Furthermore, the overall privacy guarantee can be amplified through additional stochastic techniques such as subsampling (Balle et al., 2018), iterative composition (Feldman et al., 2018), and diffusion-based mechanisms (Balle et al., 2019a). Nevertheless, theoretical privacy amplification is not guaranteed under arbitrary combinations of stochastic techniques.

Recent studies extend the notion of DP to the quantum domain, leading to Quantum Differential Privacy (QDP) (Du et al., 2021a; Hirche et al., 2023). However, several key challenges remain unaddressed. First, existing efforts primarily focus on defining privacy guarantees for quantum data. However, most practical, near-term QML applications are hybrid models that operate on classical data and use the quantum circuit only as an intermediate processing component. This hybrid architecture presents a critical privacy challenge: a DP guarantee applied only to the intermediate quantum layer does not ensure end-to-end privacy for the full model, especially if the preceding classical components are sensitive. Second, the interaction between classical noise (e.g., Gaussian, Laplacian) and intrinsic quantum noise has not yet been investigated. This research gap is critical because certain types of quantum noise, such as depolarizing noise, can naturally inject randomness into the learning process without significantly degrading the performance of models (Du et al., 2021a). This raises a crucial

¹Department of Computer & Information Science & Engineering, University of Florida, Gainesville, Florida, USA
²MITRE, Fairfax, Virginia, USA
³Department of Artificial Intelligence Convergence, Pukyong National University, Busan, South Korea
⁴Department of Education, University of Florida, Gainesville, Florida, USA. Correspondence to: My T. Thai <mythai@cise.uf.edu>.

open question: can this intrinsic quantum randomness be formally utilized as a stochastic technique to amplify the privacy guarantee originating from a preceding classical mechanism? To date, no work has theoretically established how to compose the privacy guarantees of classical and quantum noise sources within these hybrid models. In addition, understanding this relationship is crucial to control the preset privacy budget, especially considering that quantum noise in physical devices is inherently dynamic and difficult to precisely control.

Contributions. The key contributions and insights of this work can be highlighted as follows:

(i) Hybrid Privacy-Preserving Mechanism. We propose HYPER-Q, a HYbrid Privacy-presErving mechanism for Quantum Neural Networks (QNNs). To the best of our knowledge, this is the first work to investigate the joint effect of classical and quantum noise in amplifying DP within quantum hybrid models. Specifically, HYPER-Q establishes a baseline privacy guarantee via classical input perturbation (e.g., Gaussian noise), which is then theoretically amplified by quantum noise channels, with depolarizing noise as the primary focus, acting as a post-processing operation.

(ii) Privacy Guarantee Analysis. We provide a rigorous analysis of HYPER-Q’s DP guarantees. Our mechanism is a composition $Q^{(\eta)} \circ A$ where A is a classical mechanism satisfying an original (ε, δ) -DP and $Q^{(\eta)}$ is the quantum post-processing operation incorporating a depolarizing noise channel, which serves as our main analysis case. We analyze how this composition achieves new amplified privacy parameters (ε', δ') . We provide three main analytical results including two for depolarizing noise and one extension to other quantum noise channels.

- First (Theorem 4.1): We show that quantum post-processing in a d -dimensional Hilbert space acts as a privacy amplifier by strictly reducing the failure probability (achieving $\delta' = \left[\frac{\eta(1-e^\varepsilon)}{d} + (1-\eta)\delta \right]_+ < \delta$), while the privacy loss remains fixed ($\varepsilon' = \varepsilon$). This directly implies stricter certifiable adversarial robustness.
- Second (Theorem 4.4): We demonstrate that under a certain condition, it is possible to simultaneously amplify both parameters, ε' and δ' . This analysis yields two crucial insights. First, we show how to select Positive Operator-Valued Measures (POVMs) to maximize the privacy gain: the bound on δ' is minimized (i.e., the guarantee is strongest) when all POVM elements have equal trace. Second, we derive the explicit threshold that the quantum noise η must exceed to guarantee the strict amplification of both ε' and δ' .
- Third (Theorems 4.7 and 4.9): We extend the privacy analysis for depolarizing noise to other asym-

metric quantum noise channels by identifying quantum hockey-stick divergence contraction as the underlying mechanism for privacy amplification. We derive strict privacy amplification for Generalized Amplitude Damping (GAD) based on thermal relaxation ($\delta' = (2\sqrt{\eta} - \eta)\delta$) and for Generalized Dephasing (GD) under the assumption of product equatorial encoding, where the suppression of phase coherences scales the failure probability to $\delta' = |1 - 2\eta|\delta$.

(iii) Utility Analysis. We derive a formal utility bound (Theorem 4.10) that quantifies the model’s performance under the depolarizing channel. Specifically, we characterize the total error as a high-probability trade-off between the classical noise variance (σ) and the depolarizing factor (η).

(iv) Empirical Experiments. We empirically demonstrate that, under a fixed end-to-end privacy budget, HYPER-Q achieves consistently greater adversarial robustness than standard classical-only DP mechanisms across multiple datasets. These results indicate that replacing classical noise with quantum depolarizing noise can yield higher performance without weakening the privacy guarantee.

2. Preliminary

2.1. Quantum Information Basics

Qubits and States. Quantum computing systems operate on quantum bits (*qubits*). Unlike classical bits, qubits can exist in superpositions of 0 and 1. An n -qubit system resides in a 2^n -dimensional Hilbert space \mathcal{H} . While ideal (pure) states are represented by vectors $|\psi\rangle$, general (possibly noisy) states are described by density matrices ρ : $d \times d$ positive semi-definite matrices with a trace of one (i.e., $\text{Tr}[\rho] = 1$).

Quantum Channels. The evolution of a quantum state, including noise effects, is modeled by a quantum channel. For example, the depolarizing channel, denoted as $f_{\text{dep}}^{(\eta)}$, replaces the state ρ with the maximally mixed state $\frac{I}{d}$ with probability η and leaves it unchanged with probability $1 - \eta$:

$$f_{\text{dep}}^{(\eta)}(\rho) = (1 - \eta)\rho + \eta \frac{I}{d}$$

where $\eta \in [0, 1]$ is the probability, I is the identity matrix and d is the dimension of the Hilbert space.

Classical information is extracted from a quantum state via measurement. A general measurement is defined by a set of operators E_k forming a Positive Operator-Valued Measure (POVM). For a state ρ , the probability of observing the outcome k is:

$$\Pr(\text{outcome} = k) = \text{Tr}[E_k \rho].$$

2.2. Differential Privacy

Differential Privacy (DP) provides a formal guarantee that the presence or absence of any individual sample in a dataset has limited impact on the output (Dwork, 2006). More formally:

Definition 2.1 $((\varepsilon, \delta)$ -Differential Privacy). A randomized mechanism $\mathcal{M} : \mathcal{D} \rightarrow \mathcal{R}$ satisfies (ε, δ) -differential privacy if for any two adjacent datasets D_1 and D_2 that differ by a single element, , and for any subset of outputs $S \subseteq \mathcal{R}$, the following inequality holds:

$$\Pr[\mathcal{M}(D_1) \in S] \leq e^\varepsilon \Pr[\mathcal{M}(D_2) \in S] + \delta$$

,

Here, $\varepsilon \geq 0$ is the privacy loss parameter while $\delta \in [0, 1)$ is the failure probability. The smaller ε or the smaller δ implies stronger privacy.

An equivalent characterization of DP can be formulated using the **hockey-stick divergence**. For two distributions P and Q , the hockey-stick divergence is defined as:

$$D_{e^\varepsilon}(P\|Q) = \int \max(0, P(x) - e^\varepsilon Q(x)) dx$$

A mechanism \mathcal{M} satisfies (ε, δ) -DP if and only if $D_{e^\varepsilon}(\mathcal{M}(D_1)\|\mathcal{M}(D_2)) \leq \delta$ for all adjacent D_1, D_2 .

This framework extends to the quantum setting (Hirche et al., 2023), where the quantum hockey-stick divergence for states ρ, ρ' is defined as:

$$D_{e^\varepsilon}^{(q)}(\rho\|\rho') = \text{Tr}[(\rho - e^\varepsilon \rho')_+]$$

A quantum mechanism \mathcal{E} satisfies (ε, δ) -quantum DP if for any adjacent states ρ, ρ' , the divergence is bounded by δ where $D_{e^\varepsilon}^{(q)}(\mathcal{E}(\rho)\|\mathcal{E}(\rho')) \leq \delta$.

Noise-added Mechanisms. A standard way to achieve DP is by adding noise proportional to the sensitivity of a function, which is the maximum output change from altering one data point. The Gaussian mechanism adds noise $\eta_{\text{cdp}} \sim \mathcal{N}(0, \sigma^2 I)$ to a function $f : \mathcal{D} \rightarrow \mathbb{R}$ based on the function's L_2 sensitivity:

$$\Delta_2(f) = \max_{D_1, D_2} \|f(D_1) - f(D_2)\|_2$$

This mechanism outputs $f(x) + \eta_{\text{cdp}}$. For appropriate choices of σ , this mechanism satisfies (ε, δ) -DP. Additional background on hybrid quantum machine learning, and the connection between differential privacy and adversarial robustness, is provided in Appendix A.

3. Related Works

Differential Privacy in Classical Machine Learning. Differential Privacy (DP) has been established as a leading

framework for protecting data in ML workflows. DP provides formal guarantees (Dwork et al., 2006) that ensure that the inclusion or exclusion of a single data point has a limited impact on the output of an algorithm, thus minimizing the risk of information leakage. In machine learning, the most common way to achieve DP in practice is by injecting calibrated random noise into the learning process. This noise can be introduced at various stages, such as perturbing the input data (Lecuyer et al., 2019; Phan et al., 2019; Cohen et al., 2019), the gradients during optimization (Abadi et al., 2016; Ghazi et al., 2025), or the final model parameters (Yuan et al., 2023).

Input perturbation is particularly effective for providing instance-level privacy and is a key technique for certifying the adversarial robustness of a model's predictions (Lecuyer et al., 2019; Cohen et al., 2019). Standard mechanisms, such as the Gaussian or Laplacian mechanism, add noise scaled to the function's sensitivity to provide (ε, δ) -DP guarantee (Dwork & Roth, 2014). To mitigate the degradation in model performance which is often caused by noise injection, a crucial line of research focuses on privacy amplification. The core idea is that certain stochastic processes can strengthen the final privacy guarantee without requiring additional initial noise. Privacy amplification can also be achieved through established techniques such as subsampling (Bun et al., 2015; Balle et al., 2018; Wang et al., 2019; Koga et al., 2022), shuffling (Cheu et al., 2018; Erlingsson et al., 2019; Balle et al., 2019b), iterative composition (Feldman et al., 2018), and specialized forms of post-processing (Balle et al., 2019a; Ye & Shokri, 2022). In particular, post-processing is fundamental: while standard post-processing can never weaken a privacy guarantee (Dwork, 2006), certain stochastic transformations can actively enhance it. However, not all combinations of stochastic sources yield amplification. For example, post-processing a Gaussian mechanism with an additional Gaussian transformation can amplify privacy, whereas composing a Gaussian mechanism with a Laplacian transformation does not yield such an effect.

Differential Privacy in Quantum Settings. The notion of DP has recently been extended to quantum settings, reflecting the growing interest of privacy-preserving quantum computing and quantum machine learning (QML). The foundational concept was introduced by (Zhou & Ying, 2017), who proposed a definition of QDP that is a direct quantum analogue of classical DP. Building on this, (Du et al., 2021a) demonstrated a practical application for QML by showing that inherent quantum noise could be leveraged to achieve QDP in quantum classifiers. Specifically, they analyzed the depolarizing noise channel as a privacy-preserving mechanism and derived the mathematical relationship between the noise strength and the resulting (ε, δ) -QDP guarantee. They also proved that this privacy mechanism simultaneously en-

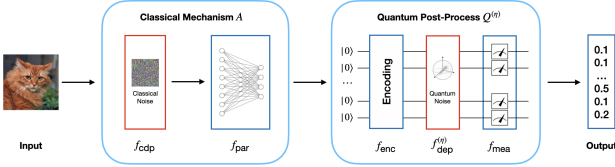


Figure 1. Overview of the proposed HYPER-Q.

hances the model’s adversarial robustness. Later, (Hirche et al., 2023) developed a comprehensive theoretical framework for QDP. Using tools such as quantum relative entropy, their work provides a more general and rigorous foundation for QDP. More recent works (Watkins et al., 2023; Bai et al., 2024; Song et al., 2025) have examined how various quantum noise sources, such as depolarizing, bit-flip, and phase-flip channels, affect the QDP budget.

Despite this progress in defining privacy for either purely quantum or purely classical systems, a critical gap remains for the hybrid quantum-classical architectures that are essential for near-term quantum advantage. These models are paramount for applying quantum computation to real-world problems. However, to date, no work has theoretically established how to compose the privacy guarantees of classical and quantum noise sources within hybrid quantum models. This significant gap highlights the importance of our proposed HYPER-Q and the need for further exploration of hybrid approaches that combine traditional DP mechanisms with the privacy properties innate to quantum systems.

4. Hybrid Noise-Added Mechanism

In this section, we present our privacy-preserving mechanism that integrates classical and quantum noise to achieve differential privacy (DP) in QNN models. We first describe the structure of the hybrid mechanism, then analyze its DP guarantees, and finally provide a utility bound that characterizes the impact of noise on model performance.

4.1. Mechanism Overview

The proposed mechanism is designed to mitigate privacy leakage at two levels. First, classical data can be vulnerable to reconstruction attacks before it enters the quantum circuit. To prevent such exposure, we introduce classical noise mechanisms to perturb the input. Second, we leverage inherent quantum depolarizing noise to enhance privacy after encoding. This noise has been shown to preserve utility in the ideal case of infinite measurements (Du et al., 2021b). By combining classical and quantum noise, our dual-layer approach reduces reliance on excessive classical noise, achieving stronger privacy with minimal utility loss.

We formally describe each stage of the mechanism using a modular function-based representation (see Figure 1):

Classical Noise Function $f_{cdp} : \mathbb{X} \rightarrow \mathbb{X}$. This function adds calibrated classical noise to the input to provide a baseline DP guarantee.

$$f_{cdp}(x) = x + \eta_{cdp}, \quad \text{where } \eta_{cdp} \sim \mathcal{N}(0, \sigma^2 I)$$

Here, the noise η_{cdp} is drawn from a multivariate Gaussian distribution with covariance $\sigma^2 I$.

Parameterized Linear Transformation $f_{par} : \mathbb{X} \rightarrow \mathbb{Y}$. This function serves as a learnable classical layer, transforming the input data into a feature space. The weights W and biases b are learnt during model training.

$$f_{par}(x') = Wx' + b = y$$

Quantum Encoding Function $f_{enc} : \mathbb{Y} \rightarrow \mathcal{H}$. This function encodes the classical feature vector y into a quantum state ρ within a d -dimensional Hilbert space \mathcal{H} composed of n qubits ($d = 2^n$). Let $|\psi_y\rangle = \prod_{j=1}^n e^{-iy_j H_j} |0\rangle^{\otimes n}$ be the encoded pure state vector, where H_j are Hermitian operators. The output is the corresponding density matrix:

$$f_{enc}(y) = |\psi_y\rangle\langle\psi_y| = \rho$$

Depolarizing Noise Channel $f_{dep}^{(\eta)} : \mathcal{H} \rightarrow \mathcal{H}$. This quantum channel adds a second layer of randomness by applying noise directly to the encoded state ρ . This process will be shown to amplify the initial privacy guarantee from the classical noise layer in the subsequent analysis.

$$f_{dep}^{(\eta)}(\rho) = (1 - \eta)\rho + \eta \frac{I}{d} = \tilde{\rho}$$

Here, $\eta \in [0, 1]$ is the depolarization probability, and I is the identity operator on \mathcal{H} .

Measurement Function $f_{mea} : \mathcal{H} \rightarrow \mathbb{Z}$. This final stage maps the noisy quantum state $\tilde{\rho}$ to a single classical class label z from the output space $\mathbb{Z} = \{0, 1, \dots, K - 1\}$. This mapping is inherently stochastic and is formally defined as:

$$\Pr(f_{mea}(\tilde{\rho}) = k) = \text{Tr}[E_k \tilde{\rho}], \quad \forall k$$

This hybrid approach allows independent tuning of classical and quantum noise for flexible privacy-utility trade-offs. Its modular design also supports theoretical analysis of privacy guarantees and performance impact, as detailed below.

4.2. Differential Privacy Bound

We now define the concepts used in our DP analysis. Specifically, our proposed mechanism can be expressed as the composition $Q^{(\eta)} \circ A$, where $A = f_{par} \circ f_{cdp}$ is a classical mechanism satisfying (ε, δ) -DP, and $Q^{(\eta)} = f_{mea} \circ f_{dep}^{(\eta)} \circ f_{enc}$ is a quantum post-processing operation controlled by a depolarizing noise parameter η . Assuming the random process

f_{cdp} satisfies (ε, δ) -DP, it follows from the post-processing theorem (Dwork, 2006) that the mechanism A also satisfies (ε, δ) -DP. While our primary focus is on depolarizing noise, the framework is modular. Replacing $f_{dep}^{(\eta)}$ with alternative quantum noise channels allows for the study of diverse quantum post-processing effects.

Our goal is to analyze how the composed mechanisms achieve new privacy parameters (ε', δ') , and how these parameters amplify the original guarantees (ε, δ) . Specifically, we present two analyses tailored to depolarizing noise, followed by a third that generalizes these results to a broader range of quantum noise channels. In the first analysis, we show that $Q^{(\eta)} \circ A$ can improve the failure probability by establishing that $\varepsilon' = \varepsilon$ and $\delta' < \delta$. In the second analysis, we demonstrate that under certain conditions, $Q^{(\eta)} \circ A$ can amplify both the privacy loss and the failure probability, achieving $\varepsilon' < \varepsilon$ and $\delta' < \delta$. In the third analysis, we extend these results beyond depolarizing noise to a broader class of channels, including Generalized Amplitude Damping (GAD) and Generalized Dephasing (GD). Through this, we identify the universal condition required for an arbitrary quantum noise channel to achieve DP amplification. All proofs and details are presented in Appendix B.

4.2.1. FIRST ANALYSIS — AMPLIFYING THE FAILURE PROBABILITY

We investigate how the failure probability is amplified under quantum post-processing, assuming a fixed privacy loss parameter ε . Theorem 4.1 formalizes this by establishing a new bound on the failure probability δ' of the composed mechanism $Q^{(\eta)} \circ A$, while keeping the privacy loss fixed at $\varepsilon' = \varepsilon$. The proof for this theorem bridges the classical and quantum divergence measures by involving two key steps: (1) establishing that the classical hockey-stick divergence of the measured probabilities is upper-bounded by the quantum hockey-stick divergence of the quantum states before measurement, and (2) proving that this quantum divergence contracts under $f_{dep}^{(\eta)}$ by a factor of $(1 - \eta)$.

Theorem 4.1 (Amplification on Failure Probability). *Let $A : \mathbb{X} \rightarrow \mathcal{P}(\mathbb{Y})$ be a classical mechanism satisfying (ε, δ) -DP where $A = f_{par} \circ f_{cdp}$, and let $Q^{(\eta)} : \mathbb{Y} \rightarrow \mathcal{P}(\mathbb{Z})$ be a quantum mechanism in a d -dimensional Hilbert space defined as $Q^{(\eta)} = f_{mea} \circ f_{dep}^{(\eta)} \circ f_{enc}$ where $0 \leq \eta \leq 1$ is the depolarizing noise factor. Then, the composed mechanism $Q^{(\eta)} \circ A$ satisfies (ε', δ') -DP, where*

$$\varepsilon' = \varepsilon, \quad \delta' = \left[\frac{\eta(1 - e^\varepsilon)}{d} + (1 - \eta)\delta \right]_+$$

It follows that for $\varepsilon \in [0, 1]$, we have $\delta' \leq \delta$. Therefore, the failure probability is strictly reduced, resulting in a privacy amplification effect, as formally stated in Corollary 4.2.

Corollary 4.2. *The composed mechanism $Q^{(\eta)} \circ A$ satisfies (ε, δ') -DP with $\delta' < \delta$, thus strictly amplifying the overall failure probability.*

Based on (Lecuyer et al., 2019), we derive an explicit condition for certifiable adversarial robustness of the composed mechanism $Q^{(\eta)} \circ A$ in Corollary 4.3. This condition defines a robustness threshold that the model's expected confidence scores must exceed. Notably, due to the privacy amplification effect formalized in Corollary 4.2, the robustness threshold under the composed mechanism (parameterized by δ') is strictly lower than that of the original classical mechanism (parameterized by δ). As a result, quantum post-processing provably enlarges the set of inputs for which adversarial robustness can be guaranteed. For further details on adversarial robustness, we refer readers to Appendix A.

Corollary 4.3. *The composed mechanism $C = Q^{(\eta)} \circ A$ is certifiably robust against adversarial perturbations for an input $x \in \mathbb{X}$ if this condition holds for the correct class k :*

$$\mathbb{E}[[C(x)]_k] > e^{2\varepsilon} \max_{i \neq k} \mathbb{E}[[C(x)]_i] + (1 + e^\varepsilon)\delta'$$

4.2.2. SECOND ANALYSIS — AMPLIFYING THE PRIVACY LOSS

We investigate how the composed mechanism $Q^{(\eta)} \circ A$ can simultaneously amplify both the privacy loss ε and the failure probability δ . The result is formalized in Theorem 4.4 which provides new (ε', δ') bound. The proof (detailed in Appendix B) relies on the *Advanced Joint Convexity* theory, originally introduced in (Balle et al., 2018). The key insight is that the depolarizing channel transforms the final output distribution into a convex combination of the original (noiseless) distribution and the distribution of a maximally mixed state. This explicit mixture structure allows the joint convexity theorem to be applied, yielding a new DP bound on both privacy loss and failure probability.

Theorem 4.4 reveals that the amplified failure probability δ' depends on the choice of POVMs. In particular, δ' becomes tighter as $\varphi = \min_k \left(\frac{\text{Tr}(E_k)}{d} \right)$ increases. This insight leads to Corollary 4.5, highlighting that δ' is minimized when all POVM elements E_k have equal trace (i.e., $\text{Tr}(E_k) = \frac{1}{K}$).

Contrarily, $\varepsilon' \leq \varepsilon$ for all $\eta \in [0, 1]$, the privacy loss in terms of ε is always reduced. However, the bound on δ is only improved (i.e., $\delta' \leq \delta$) when the noise level η exceeds the threshold given in Corollary 4.6. This condition shows that a sufficient level of quantum noise is required to achieve strict amplification of the privacy guarantee in both parameters.

Theorem 4.4 (Amplification on Privacy Loss). *Let $A = f_{par} \circ f_{cdp}$ be (ε, δ) -DP, and $Q^{(\eta)} = f_{mea} \circ f_{dep}^{(\eta)} \circ f_{enc}$ be a quantum mechanism in a d -dimensional Hilbert space*

where $0 \leq \eta \leq 1$ is the depolarizing noise factor. Then, the composition $Q^{(\eta)} \circ A$ is (ε', δ') -DP where $\varepsilon' = \log(1 + (1 - \eta)(e^\varepsilon - 1))$ and $\delta' = (1 - \eta)(1 - e^{\varepsilon' - \varepsilon}(1 - \delta) - (e^\varepsilon - e^{\varepsilon'})\varphi)$ with $\varphi = \min_k \left(\frac{\text{Tr}(E_k)}{d} \right)$.

Corollary 4.5. Let $\{E_k\}_{k=1}^K$ be the POVM used in f_{mea} . Then, the amplified failure probability δ' in Theorem 4.4 is minimized when all POVM elements have equal trace (i.e., $\text{Tr}[E_k] = \frac{d}{K}$ for all $k \in \{1, \dots, K\}$).

Corollary 4.6. Given an optimal measurement such that $\text{Tr}[E_k] = \frac{d}{K} \forall k$, the composed mechanism $Q^{(\eta)} \circ A$ strictly improves the privacy guarantee (i.e., $\varepsilon' \leq \varepsilon$ and $\delta' \leq \delta$) if

$$\eta \geq 1 - \frac{\delta}{(1 - \delta)(1 - e^{-\varepsilon}) - (e^\varepsilon - 1)/K}$$

4.2.3. THIRD ANALYSIS — EXTENDING TO OTHER QUANTUM NOISE CHANNELS

While our two first analyses focus on depolarizing noise, the underlying mechanism responsible for privacy amplification extends naturally to a broader class of quantum channels. The central insight is whenever a quantum noise channel induces a non-trivial contraction of the quantum hockey-stick divergence, it will inherently lead to privacy amplification. In this subsection, we show how this principle generalizes our first analysis to two widely studied asymmetric noise channels: Generalized Amplitude Damping (GAD) and Generalized Dephasing (GD). A more detailed discussion is provided in Appendix B.4.

Amplification Under Generalized Amplitude Damping. GAD channel is inherently asymmetric and non-unital. Despite this, we show that it contracts trace distance by a factor of at most $(2\sqrt{\eta} - \eta)$, where η is the damping strength of GAD channel. Substituting this contraction into the proof framework for Theorem 4.1 yields the following (ε', δ') .

Theorem 4.7 (Amplification Under Generalized Amplitude Damping Noise). *Let $A : \mathbb{X} \rightarrow \mathcal{P}(\mathbb{Y})$ be a classical mechanism satisfying (ε, δ) -DP where $A = f_{\text{par}} \circ f_{\text{cdp}}$, and let $Q^{(p, \eta)} : \mathbb{Y} \rightarrow \mathcal{P}(\mathbb{Z})$ be a quantum mechanism in d -dimensional Hilbert space defined as $Q^{(p, \eta)} = f_{\text{mea}} \circ f_{\text{GAD}}^{(p, \eta)} \circ f_{\text{enc}}$. Then, the composed mechanism $Q^{(p, \eta)} \circ A$ satisfies (ε', δ') -DP, where*

$$\varepsilon' = \varepsilon, \quad \delta' = (2\sqrt{\eta} - \eta)\delta.$$

Generalized Dephasing Under Equatorial Encoding. Dephasing noise preserves classical populations but suppresses quantum coherences. Although its worst-case contraction coefficient is 1, we show that for many QML encoding schemes, including angle-based encoders, the encoded states

lie in the equatorial plane of the Bloch sphere. Under this structure, all distinguishability is encoded in coherence terms directly affected by GD noise, enabling nontrivial contraction.

Assumption 4.8 (Product Equatorial Encoding on All Qubits). For each input $y \in \mathbb{Y}$, the encoder prepares a product state

$$\rho_y = f_{\text{enc}}(y) = \bigotimes_{j=1}^n \rho_y^{(j)},$$

where each single-qubit factor $\rho_y^{(j)}$ is an equatorial state on the Bloch sphere, i.e.,

$$\rho_y^{(j)} = \frac{1}{2} \left(I + \cos \phi_y^{(j)} X + \sin \phi_y^{(j)} Y \right),$$

for some angle $\phi_y^{(j)} \in \mathbb{R}$ and with no Z -component.

Under this assumption, the GD channel contracts all relevant coherence terms by a factor of $|1 - 2\eta|$ where η is the dephasing parameter of the GD channel, leading to the following privacy guarantee.

Theorem 4.9. *Let $A : \mathbb{X} \rightarrow \mathcal{P}(\mathbb{Y})$ be a classical mechanism satisfying (ε, δ) -DP, and let*

$$Q^{(\eta)} := f_{\text{mea}} \circ f_{\text{GD}}^{(\eta)} \circ f_{\text{enc}}$$

be an n -qubit quantum mechanism where $f_{\text{GD}}^{(\eta)}$ is the n -qubit GD channel and f_{enc} satisfies Assumption 4.8. Then the composed mechanism $Q^{(\eta)} \circ A$ satisfies (ε', δ') -DP with

$$\varepsilon' = \varepsilon, \quad \delta' = |1 - 2\eta| \cdot \delta.$$

4.3. Utility Bound

We finally establish a rigorous framework to study the utility loss, defined as the absolute error between the noisy and noise-free versions of our mechanism. The final output of the mechanism is stochastic, due to the sampling-based measurement process. Thus, we analyze the difference between the expected values of their output. The expected value represents the average behavior of a mechanism and provides a deterministic quantity that we can use to measure utility loss.

Formally, we define the expectation measurement function $f_{\text{exp}} : \mathcal{H} \rightarrow \mathbb{R}$ as:

$$f_{\text{exp}}(\rho) = \sum_k k \text{Tr}[E_k \rho] = \text{Tr}[E_{\text{exp}} \rho]$$

where $E_{\text{exp}} = \sum_k k E_k$ is the expectation value observable.

Using this function, we define our deterministic expectation mechanisms. The **full mechanism**, including classical and

quantum noise, is $\mathcal{M}_{\text{full}}(x) = (f_{\text{exp}} \circ f_{\text{dep}}^{(\eta)} \circ f_{\text{enc}} \circ f_{\text{par}} \circ f_{\text{cdp}})(x)$. On the other hand, the **noise-free mechanism (clean)** is $\mathcal{M}_{\text{clean}}(x) = (f_{\text{exp}} \circ f_{\text{enc}} \circ f_{\text{par}})(x)$. The total utility loss is the worst-case absolute error between their expected outputs:

$$\text{Error} = \sup_{x \in \mathbb{X}} |\mathcal{M}_{\text{full}}(x) - \mathcal{M}_{\text{clean}}(x)|$$

Theorem 4.10 (Utility Bound). *Let the classical noise be $\kappa \sim \mathcal{N}(0, \sigma^2 I)$ acting on an input space \mathbb{X} of dimension $d_X = \dim(\mathbb{X})$. For any desired failure probability $p > 0$, the utility loss is bounded probabilistically as:*

$$\Pr \left(\text{Error} \leq L_\infty \cdot \sigma \sqrt{2 \ln \frac{2d_X}{p} + 2\eta \|E_{\text{exp}}\|_{\text{op}}} \right) \geq 1 - p$$

$$\text{where } L_\infty = 2(1 - \eta) \|E_{\text{exp}}\|_{\text{op}} \|W\|_\infty \left(\sum_j \|H_j\|_{\text{op}} \right).$$

Theorem 4.10 provides a utility bound that quantifies the trade-off between privacy and performance. The proof (detailed in Appendix B) utilizes an **intermediate mechanism (half)** that includes only quantum noise as $\mathcal{M}_{\text{half}}(x) = (f_{\text{exp}} \circ f_{\text{dep}}^{(\eta)} \circ f_{\text{enc}} \circ f_{\text{par}})(x)$. Specifically, first, we bound the error introduced by the quantum noise ($|\mathcal{M}_{\text{half}} - \mathcal{M}_{\text{clean}}|$), which is shown to be proportional to the quantum noise level η . Second, we bound the error from the classical noise by establishing a Lipschitz constant L_∞ for the quantum-only mechanism. As the classical noise is unbounded, the final guarantee is a high-probability statement relating the utility loss to the classical (σ) and quantum (η) noise levels.

5. Experimental Evaluation

In this section, we empirically evaluate HYPER-Q, focusing on adversarial robustness, a direct outcome of the DP guarantee in Corollary 4.3. First, we conduct a sensitivity analysis of the depolarizing noise parameter η to identify the optimal balance between quantum distortion and privacy amplification. Then, we show that given a fixed privacy budget (ε', δ') , HYPER-Q is more efficient for QML models than existing DP mechanisms.

Implementation Details. We implement a QML model designed to incorporate HYPER-Q. In the QML architecture, the variational quantum circuit uses 5-10 qubits and consists of three alternating layers of single-qubit RX rotations and entangling layers, corresponding to the encoding function f_{enc} . Entanglement is implemented via a circular pattern of CNOT gates, followed by computational-basis projective measurement and a final fully connected layer to produce the prediction. This architecture widely adopted in prior QML and QDP studies (Havlíček et al., 2019; Du et al., 2021a; Watkins et al., 2023; Long et al., 2025). The implementation uses the PennyLane library (Bergholm et al.,

2022), with quantum circuits executed on simulators, which is a standard practice for prototyping and evaluating quantum applications (Cicero et al., 2025). To ensure DP, Gaussian noise is added directly to the input and depolarizing noise is applied as a layer in the quantum circuit. Specifically, given a target privacy budget (ε', δ') , the depolarizing noise level η is fixed, while the Gaussian noise level σ^2 is computed according to Theorem 4.1. Further details and justification are provided in Appendix C.

Datasets and Baselines. We evaluate our approach on three standard image classification datasets: MNIST (Lecun et al., 1998), FashionMNIST (Xiao et al., 2017), and USPS (Hull, 2002). We compare HYPER-Q against classical DP mechanisms including Basic Gaussian, Analytic Gaussian (Balle & Wang, 2018) and DP-SGD (Abadi et al., 2016; Watkins et al., 2023). We note that the first two mechanisms apply noise at the input level, whereas DP-SGD performs noise injection at the gradient level of the QML model. Each experiment reports the averaged accuracy over 10 runs. More details are provided in Appendix D.

Adversarial Robustness Settings. We use a certified defense framework (Lecuyer et al., 2019) that trains models with noise layers calibrated by a DP budget (ε', δ') and a construction attack bound L_{cons} . We then evaluate robustness by measuring the model's accuracy against FGSM (Goodfellow et al., 2015) and PGD (Madry et al., 2018) attacks, whose strength is defined by the empirical attack bound L_{attk} . More details are provided in Appendix E.

5.1. Sensitivity Analysis of η

To characterize the impact of the depolarizing parameter on model utility, we evaluate model accuracy across varying levels of depolarizing noise $\eta \in \{0.05, 0.1, \dots, 0.4\}$. For each noise level η , we measured robustness against FGSM attacks with varying strengths $L_{\text{attk}} \in \{0, 0.01, \dots, 0.05\}$. We conducted these experiments across three datasets (MNIST, Fashion-MNIST, and USPS) under four distinct differential privacy guarantees $\varepsilon' \in \{0.25, 0.5, 0.75, 1\}$.

As illustrated in Figure 2, the relationship between η and model accuracy exhibits a remarkably consistent unimodal structure across all evaluated settings. The accuracy curves follow a shared pattern. Specifically, utility initially increases as η rises. This trend is driven by the ability of quantum noise to offload the requirement for disruptive classical Gaussian noise. Then, utility reaches a peak for $\eta = 0.1$ with $\varepsilon' \leq 0.5$ and $\eta = 0.05$ with $\varepsilon' > 0.5$. Finally, utility declines as the quantum distortion overwhelms the underlying data signal. Our sensitivity analysis reveals stable trends that provide a robust heuristic for depolarizing noise calibration. First, the optimal value for η consistently falls within the narrow interval of $[0.05, 0.15]$ across all privacy budgets and attack strengths. Additionally, more relaxed

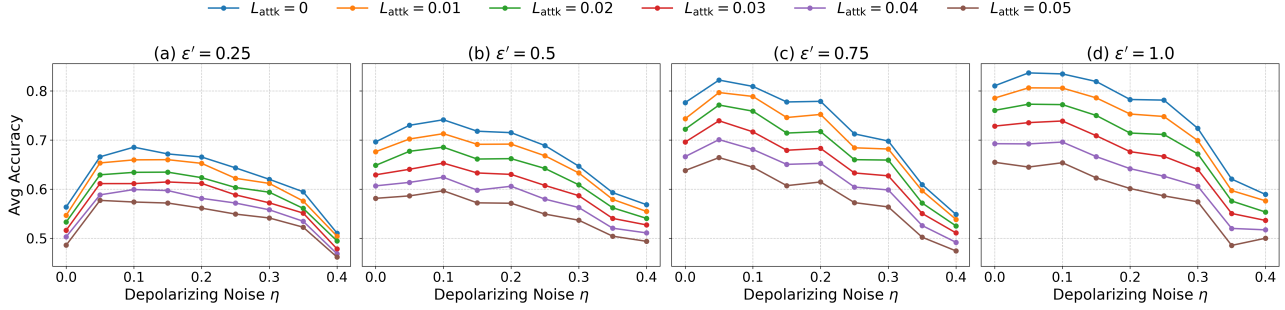


Figure 2. Subplots (a)–(d) illustrate the trade-off between quantum noise and model accuracy across MNIST, FashionMNIST, and USPS for privacy budgets $\varepsilon' \in \{0.25, 0.5, 0.75, 1.0\}$. Each curve denotes the mean accuracy under FGSM attacks of varying strengths (L_{attk}).

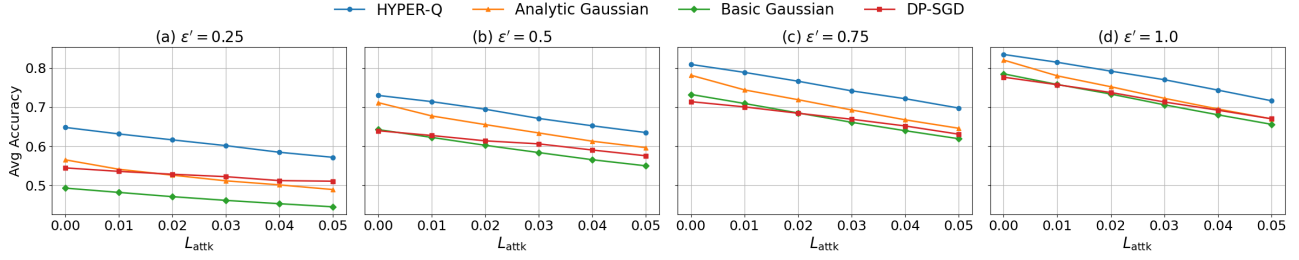


Figure 3. Average accuracy of noise-added mechanisms under FGSM and PGD attacks on MNIST, FashionMNIST, and USPS. Accuracy is averaged over all L_{cons} settings for each $(L_{\text{attk}}, \varepsilon')$. HYPER-Q is evaluated with $\eta = 0.1$ and $\delta' = 1 \times 10^{-5}$.

privacy budgets generally require smaller values of η for optimal results. More details are provided in Appendix F.1.

5.2. Robustness Analysis of HYPER-Q

In this experiment, we illustrate that under the same privacy budget, HYPER-Q preserves adversarial robustness more efficiently than classical mechanisms in QML. We evaluate the adversarial robustness of HYPER-Q under the depolarizing noise $\eta = 0.1$ which is selected based on our sensitivity analysis. We compare its performance with Basic Gaussian, Analytic Gaussian and DP-SGD mechanisms. For fair comparisons, we ensure that all methods are evaluated under the same privacy budget and applied to the same QML model.

Figure 3 presents the average accuracy on the MNIST, FashionMNIST, and USPS datasets under both FGSM and PGD attacks for four distinct privacy budgets $\varepsilon' \in \{0.25, 0.5, 0.75, 1\}$. We observe that HYPER-Q consistently outperforms all baseline methods, both in the absence of attack ($L_{\text{attk}} = 0$) and under attack ($L_{\text{attk}} > 0$). As the ε' increases, the performance gap becomes more pronounced. Specifically, HYPER-Q surpasses the second-best method, Analytic Gaussian, by an average of 16.54%, 5.37%, 6.44%, and 5.20% in accuracy across the four respective ε' values. This demonstrates that replacing a reasonable amount of classical noise with quantum noise can enhance adversarial accuracy. More details are provided in Appendix F.2.

For a complete evaluation, we refer readers to additional experimental studies in the Appendix, including: (i) a comparative benchmark against classical ML models, where the QML model equipped with HYPER-Q is compared to classical models protected by classical DP mechanisms (Appendix F.3); (ii) an analysis of dimensional scalability (Appendix F.4); (iii) an empirical verification of the tightness of the utility bound in Theorem 4.10 (Appendix F.5); and (iv) an evaluation on the CIFAR-10 dataset (Appendix F.6).

6. Conclusion

In this work we have presented HYPER-Q as a hybrid privacy-preserving mechanism for quantum systems. Through extensive experimental analyses across three real-world datasets subjected to the FGSM and PGD attacks, we demonstrate that the combination of quantum and classical noise is both robust and scalable, while yielding notable improvements in privacy preservation and utility. Classical components ensure stable training and feasibility in interpretation, while quantum noise introduces natural randomness that enhances privacy without heavily degrading utility. As quantum hardware matures, we expect frameworks like HYPER-Q to be essential in shaping the future of privacy-preserving ML. A core direction for future work is to investigate the behavior of hybrid DP mechanisms on larger variational circuits deployed on actual quantum hardware.

Impact Statement

This paper presents work whose goal is to advance the field of machine learning. There are many potential societal consequences of our work, none of which we feel must be specifically highlighted here.

References

Abadi, M., Chu, A., Goodfellow, I., McMahan, H. B., Mironov, I., Talwar, K., and Zhang, L. Deep learning with differential privacy. In *Proceedings of the 2016 ACM SIGSAC conference on computer and communications security*, pp. 308–318, 2016.

Bai, Y.-R., Tao, Y.-H., Wu, S.-H., Zhang, H., and Fei, S.-M. Quantum differential privacy under noise channels. *Physica Scripta*, 99(3):035119, 2024.

Balle, B. and Wang, Y.-X. Improving the Gaussian mechanism for differential privacy: Analytical calibration and optimal denoising. In Dy, J. and Krause, A. (eds.), *Proceedings of the 35th International Conference on Machine Learning*, volume 80 of *Proceedings of Machine Learning Research*, pp. 394–403. PMLR, 10–15 Jul 2018. URL <https://proceedings.mlr.press/v80/balle18a.html>.

Balle, B., Barthe, G., and Gaboardi, M. Privacy amplification by subsampling: tight analyses via couplings and divergences. In *Proceedings of the 32nd International Conference on Neural Information Processing Systems*, NIPS’18, pp. 6280–6290, Red Hook, NY, USA, 2018. Curran Associates Inc.

Balle, B., Barthe, G., Gaboardi, M., and Geumlek, J. Privacy amplification by mixing and diffusion mechanisms. In *Neural Information Processing Systems*, 2019a. URL <https://api.semanticscholar.org/CorpusID:168170121>.

Balle, B., Bell, J., Gascón, A., and Nissim, K. The privacy blanket of the shuffle model. In *Advances in Cryptology – CRYPTO 2019: 39th Annual International Cryptology Conference, Santa Barbara, CA, USA, August 18–22, 2019, Proceedings, Part II*, pp. 638–667, Berlin, Heidelberg, 2019b. Springer-Verlag. ISBN 978-3-030-26950-0. doi: 10.1007/978-3-030-26951-7_22. URL https://doi.org/10.1007/978-3-030-26951-7_22.

Berberich, J., Fink, D., and Holm, C. Robustness of quantum algorithms against coherent control errors. *Phys. Rev. A*, 109:012417, Jan 2024. doi: 10.1103/PhysRevA.109.012417. URL <https://link.aps.org/doi/10.1103/PhysRevA.109.012417>.

Bergholm, V., Izaac, J., Schuld, M., Gogolin, C., Ahmed, S., Ajith, V., Alam, M. S., Alonso-Linaje, G., Akash-Narayanan, B., Asadi, A., Arrazola, J. M., Azad, U., Banning, S., Blank, C., Bromley, T. R., Cordier, B. A., Ceroni, J., Delgado, A., Matteo, O. D., Dusko, A., Garg, T., Guala, D., Hayes, A., Hill, R., Ijaz, A., Isacsson, T., Ittah, D., Jahangiri, S., Jain, P., Jiang, E., Khandelwal, A., Kottmann, K., Lang, R. A., Lee, C., Loke, T., Lowe, A., McKiernan, K., Meyer, J. J., Montañez-Barrera, J. A., Moyard, R., Niu, Z., O’Riordan, L. J., Oud, S., Panigrahi, A., Park, C.-Y., Polatajko, D., Quesada, N., Roberts, C., Sá, N., Schoch, I., Shi, B., Shu, S., Sim, S., Singh, A., Strandberg, I., Soni, J., Száva, A., Thabet, S., Vargas-Hernández, R. A., Vincent, T., Vitucci, N., Weber, M., Wierichs, D., Wiersema, R., Willmann, M., Wong, V., Zhang, S., and Killoran, N. PennyLane: Automatic differentiation of hybrid quantum-classical computations, 2022. URL <https://arxiv.org/abs/1811.04968>.

Bun, M., Nissim, K., Stemmer, U., and Vadhan, S. P. Differentially private release and learning of threshold functions. In *2015 IEEE 56th Annual Symposium on Foundations of Computer Science*, pp. 634–649, 2015. URL <https://api.semanticscholar.org/CorpusID:3338015>.

Cheu, A., Smith, A. D., Ullman, J., Zeber, D., and Zhilyaev, M. Distributed differential privacy via shuffling. *IACR Cryptol. ePrint Arch.*, 2019:245, 2018. URL <https://api.semanticscholar.org/CorpusID:54464170>.

Cicero, A., Maleki, M. A., Azhar, M. W., Kockum, A. F., and Trancoso, P. Simulation of quantum computers: Review and acceleration opportunities. *ACM Transactions on Quantum Computing*, September 2025. doi: 10.1145/3762672. URL <https://doi.org/10.1145/3762672>. Just Accepted.

Cohen, J., Rosenfeld, E., and Kolter, Z. Certified adversarial robustness via randomized smoothing. In Chaudhuri, K. and Salakhutdinov, R. (eds.), *Proceedings of the 36th International Conference on Machine Learning*, volume 97 of *Proceedings of Machine Learning Research*, pp. 1310–1320. PMLR, 09–15 Jun 2019. URL <https://proceedings.mlr.press/v97/cohen19c.html>.

Cullen, A. C., Montague, P., Liu, S., Erfani, S. M., and Rubinstein, B. I. P. It’s Simplex! Disaggregating Measures to Improve Certified Robustness. In *2024 IEEE Symposium on Security and Privacy (SP)*, pp. 2886–2900, Los Alamitos, CA, USA, May 2024. IEEE Computer Society. doi: 10.1109/SP54263.2024.00065. URL <https://doi.ieee.org/10.1109/SP54263.2024.00065>.

Dong, J., Roth, A., and Su, W. J. Gaussian differential privacy. *Journal of the Royal Statistical Society Series B: Statistical Methodology*, 84(1):3–37, 2022.

Dosovitskiy, A., Beyer, L., Kolesnikov, A., Weissenborn, D., Zhai, X., Unterthiner, T., Dehghani, M., Minderer, M., Heigold, G., Gelly, S., et al. An image is worth 16x16 words: Transformers for image recognition at scale. In *International Conference on Learning Representations*, 2021.

Du, Y., Hsieh, M.-H., Liu, T., Tao, D., and Liu, N. Quantum noise protects quantum classifiers against adversaries. *Phys. Rev. Res.*, 3:023153, May 2021a.

Du, Y., Hsieh, M.-H., Liu, T., Tao, D., and Liu, N. Quantum noise protects quantum classifiers against adversaries. *Phys. Rev. Res.*, 3:023153, May 2021b. doi: 10.1103/PhysRevResearch.3.023153. URL <https://link.aps.org/doi/10.1103/PhysRevResearch.3.023153>.

Dwork, C. Differential privacy. In *International Colloquium on Automata, Languages and Programming*, 2006. URL <https://api.semanticscholar.org/CorpusID:2565493>.

Dwork, C. and Roth, A. The algorithmic foundations of differential privacy. *Found. Trends Theor. Comput. Sci.*, 9(3–4):211–407, August 2014. ISSN 1551-305X. doi: 10.1561/0400000042. URL <https://doi.org/10.1561/0400000042>.

Dwork, C., McSherry, F., Nissim, K., and Smith, A. Calibrating noise to sensitivity in private data analysis. In *Theory of cryptography conference*, pp. 265–284. Springer, 2006.

Erlingsson, U., Feldman, V., Mironov, I., Raghunathan, A., Talwar, K., and Thakurta, A. Amplification by shuffling: from local to central differential privacy via anonymity. In *Proceedings of the Thirtieth Annual ACM-SIAM Symposium on Discrete Algorithms*, SODA ’19, pp. 2468–2479, USA, 2019. Society for Industrial and Applied Mathematics.

Feldman, V., Mironov, I., Talwar, K., and Thakurta, A. Privacy amplification by iteration. *2018 IEEE 59th Annual Symposium on Foundations of Computer Science (FOCS)*, pp. 521–532, 2018. URL <https://api.semanticscholar.org/CorpusID:52055752>.

Fisher, K. A. G., Broadbent, A., Shalm, L. K., Yan, Z., Lavoie, J., Prevedel, R., Jennewein, T., and Resch, K. J. Quantum computing on encrypted data. *Nature Communications*, 5(1):3074, Jan 2014. ISSN 2041-1723. doi: 10.1038/ncomms4074. URL <https://doi.org/10.1038/ncomms4074>.

Geng, Q. and Viswanath, P. The optimal noise-adding mechanism in differential privacy. *IEEE Transactions on Information Theory*, 62:925–951, 2012. URL <https://api.semanticscholar.org/CorpusID:8989005>.

Ghazi, B., Guzmán, C., Kamath, P., Kumar, R., and Manurangsi, P. Differentially private optimization with sparse gradients. In *Proceedings of the 38th International Conference on Neural Information Processing Systems*, NIPS ’24, Red Hook, NY, USA, 2025. Curran Associates Inc. ISBN 9798331314385.

Goodfellow, I. J., Shlens, J., and Szegedy, C. Explaining and harnessing adversarial examples. *International Conference on Learning Representations*, 2015.

Hatakeyama-Sato, K., Igarashi, Y., Kashikawa, T., Kimura, K., and Oyaizu, K. Quantum circuit learning as a potential algorithm to predict experimental chemical properties. *Digital Discovery*, 2:165–176, 2023. doi: 10.1039/D2DD00090C. URL <http://dx.doi.org/10.1039/D2DD00090C>.

Havlíček, V., Cárocoles, A. D., Temme, K., Harrow, A. W., Kandala, A., Chow, J. M., and Gambetta, J. M. Supervised learning with quantum-enhanced feature spaces. *Nature*, 567(7747):209–212, Mar 2019. ISSN 1476-4687. doi: 10.1038/s41586-019-0980-2. URL <https://doi.org/10.1038/s41586-019-0980-2>.

He, K., Zhang, X., Ren, S., and Sun, J. Deep residual learning for image recognition. In *Proceedings of the IEEE conference on computer vision and pattern recognition*, pp. 770–778, 2016.

Hirche, C. Quantum doeblin coefficients: A simple upper bound on contraction coefficients. In *2024 IEEE International Symposium on Information Theory (ISIT)*, pp. 557–562, 2024. doi: 10.1109/ISIT57864.2024.10619667.

Hirche, C., Rouzé, C., and França, D. S. Quantum differential privacy: An information theory perspective. *IEEE Transactions on Information Theory*, 69(9):5771–5787, 2023. doi: 10.1109/TIT.2023.3272904.

Hu, Z., Wolle, R., Tian, M., Guan, Q., Humble, T., and Jiang, W. Toward consistent high-fidelity quantum learning on unstable devices via efficient in-situ calibration. In Muller, H., Alexev, Y., Delgado, A., and Byrd, G. (eds.), *Proceedings - 2023 IEEE International Conference on Quantum Computing and Engineering, QCE 2023*, Proceedings - 2023 IEEE International Conference on Quantum Computing and Engineering, QCE 2023, pp. 848–858. Institute of Electrical and Electronics Engineers Inc., 2023. doi: 10.1109/QCE57702.2023.00099. Publisher Copyright: © 2023 IEEE.; 4th IEEE International Conference

on Quantum Computing and Engineering, QCE 2023 ; Conference date: 17-09-2023 Through 22-09-2023.

Hull, J. J. A database for handwritten text recognition research. *IEEE Transactions on pattern analysis and machine intelligence*, 16(5):550–554, 2002.

Hur, T., Kim, L., and Park, D. K. Quantum convolutional neural network for classical data classification. *Quantum Machine Intelligence*, 4(1):3, Feb 2022. ISSN 2524-4914. doi: 10.1007/s42484-021-00061-x. URL <https://doi.org/10.1007/s42484-021-00061-x>.

Ji, T. and Li, P. Less is more: revisiting the gaussian mechanism for differential privacy. In *Proceedings of the 33rd USENIX Conference on Security Symposium*, SEC ’24, USA, 2024. USENIX Association. ISBN 978-1-939133-44-1.

Koga, T., Meehan, C., and Chaudhuri, K. Privacy amplification by subsampling in time domain. In Camps-Valls, G., Ruiz, F. J. R., and Valera, I. (eds.), *Proceedings of The 25th International Conference on Artificial Intelligence and Statistics*, volume 151 of *Proceedings of Machine Learning Research*, pp. 4055–4069. PMLR, 28–30 Mar 2022. URL <https://proceedings.mlr.press/v151/koga22a.html>.

Lecun, Y., Bottou, L., Bengio, Y., and Haffner, P. Gradient-based learning applied to document recognition. *Proceedings of the IEEE*, 86(11):2278–2324, 1998. doi: 10.1109/5.726791.

Lecuyer, M., Atlidakis, V., Geambasu, R., Hsu, D., and Jana, S. Certified robustness to adversarial examples with differential privacy. In *2019 IEEE Symposium on Security and Privacy (SP)*, pp. 656–672, 2019. doi: 10.1109/SP.2019.00044.

Long, C., Huang, M., Ye, X., Futamura, Y., and Sakurai, T. Hybrid quantum-classical-quantum convolutional neural networks. *Scientific Reports*, 15(1):31780, Aug 2025. ISSN 2045-2322. doi: 10.1038/s41598-025-13417-1. URL <https://doi.org/10.1038/s41598-025-13417-1>.

Madry, A., Makelov, A., Schmidt, L., Tsipras, D., and Vladu, A. Towards deep learning models resistant to adversarial attacks. In *International Conference on Learning Representations*, 2018.

Melo, A., Earnest-Noble, N., and Tacchino, F. Pulse-efficient quantum machine learning. *Quantum*, 7:1130, October 2023. ISSN 2521-327X. doi: 10.22331/q-2023-10-09-1130. URL <https://doi.org/10.22331/q-2023-10-09-1130>.

Nielsen, M. A. and Chuang, I. L. *Quantum Computation and Quantum Information: 10th Anniversary Edition*. Cambridge University Press, 2010.

Pérez-Salinas, A., Cervera-Lierta, A., Gil-Fuster, E., and Latorre, J. I. Data re-uploading for a universal quantum classifier. *Quantum*, 4:226, February 2020. ISSN 2521-327X. doi: 10.22331/q-2020-02-06-226. URL <https://doi.org/10.22331/q-2020-02-06-226>.

Phan, H., Thai, M. T., Hu, H., Jin, R., Sun, T., and Dou, D. Scalable differential privacy with certified robustness in adversarial learning. In *International Conference on Machine Learning*, 2019. URL <https://api.semanticscholar.org/CorpusID:219558337>.

Schuld, M. and Killoran, N. Quantum machine learning in feature hilbert spaces. *Phys. Rev. Lett.*, 122:040504, Feb 2019. doi: 10.1103/PhysRevLett.122.040504. URL <https://link.aps.org/doi/10.1103/PhysRevLett.122.040504>.

Song, B., Pokhrel, S. R., Vasilakos, A. V., Zhu, T., and Li, G. Towards a hybrid quantum differential privacy. *IEEE Journal on Selected Areas in Communications*, 2025.

Wang, Y.-X., Balle, B., and Kasiviswanathan, S. P. Subsampled rényi differential privacy and analytical moments accountant. In *The 22nd international conference on artificial intelligence and statistics*, pp. 1226–1235. PMLR, 2019.

Watkins, W. M., Chen, S. Y.-C., and Yoo, S. Quantum machine learning with differential privacy. *Scientific Reports*, 13(1):2453, 2023.

Xiao, H., Rasul, K., and Vollgraf, R. Fashion-mnist: a novel image dataset for benchmarking machine learning algorithms. *arXiv preprint arXiv:1708.07747*, 2017.

Xiao, X., Yao, Y., Zhou, L.-M., and Wang, X. Distribution of quantum fisher information in asymmetric cloning machines. *Scientific Reports*, 4(1):7361, Dec 2014. ISSN 2045-2322. doi: 10.1038/srep07361. URL <https://doi.org/10.1038/srep07361>.

Ye, J. and Shokri, R. Differentially private learning needs hidden state (or much faster convergence). In Koyejo, S., Mohamed, S., Agarwal, A., Belgrave, D., Cho, K., and Oh, A. (eds.), *Advances in Neural Information Processing Systems*, volume 35, pp. 703–715. Curran Associates, Inc., 2022.

Yuan, X., Ni, W., Ding, M., Wei, K., Li, J., and Poor, H. V. Amplitude-varying perturbation for balancing privacy and utility in federated learning. *IEEE Transactions on Information Forensics and Security*, 18:1884–1897, 2023. doi: 10.1109/TIFS.2023.3258255.

Zhou, L. and Ying, M. Differential privacy in quantum computation. In *2017 IEEE 30th Computer Security Foundations Symposium (CSF)*, pp. 249–262, 2017. doi: 10.1109/CSF.2017.23.

Appendix

A. Additional Background

A.1. Quantum Neural Networks

Quantum neural networks (QNNs) are a class of quantum machine learning models that employ parameterized quantum circuits to learn from classical or quantum data. In this work, we focus on QNNs designed for classical input. In a supervised learning context, a QNN aims to approximate an unknown function $K : \mathbb{X} \rightarrow \mathbb{Y}$ by training on a dataset $S = \{(x_i, y_i)\}_{i=1}^N$, where each $x_i \in \mathbb{R}^d$ is an input data vector and y_i is the associated label.

QNN models use parameterized quantum circuits to process data. The workflow for a typical QNN involves:

- **Data Encoding:** Classical data is mapped into the quantum state of qubits using a parameterized "encoder" circuit. This step is crucial, as it can be trained to find powerful data representations and can introduce quantum features like entanglement to increase the model's capacity.
- **Model Circuit:** A sequence of parameterized quantum gates, analogous to the layers of a classical neural network, processes the encoded quantum state.
- **Measurement:** A measurement is performed on the final state to extract a classical output, which serves as the model's prediction.

Training a QNN is a hybrid quantum-classical process. The quantum computer executes the circuit and performs the measurement. A classical computer then calculates a loss function (e.g., Mean Squared Error) to quantify the error between the prediction and the true label. Given a differentiable loss function $f(\cdot)$, the objective is to minimize:

$$\mathcal{L}(\theta) = \sum_{i=1}^N f(\ell_i(\theta; y_i), y_i).$$

Finally, the classical computer uses gradient-based optimization to update the circuit's parameters, θ . This process is repeated iteratively until the model converges. The goal is to find the optimal parameters θ^* that minimize the loss:

$$\theta^* = \arg \min_{\theta} \mathcal{L}(\theta).$$

A.2. Adversarial Robustness

A model is considered *adversarially robust* if it can consistently make correct predictions even when its inputs are slightly altered by malicious perturbations. These altered inputs are known as *adversarial samples*. Formally, we define a model $f : \mathbb{X} \rightarrow \mathbb{Y}$, which maps an input in the space \mathbb{X} to an output distribution over labels $y = \{y_1, y_2, \dots, y_k\} \in \mathbb{Y}$. The model f is considered adversarially robust if its prediction for an input x is unchanged when a small perturbation α is added to x . This can be stated as:

$$\max_{i \in [1, k]} [f(x)]_i = \max_{i \in [1, k]} [f(x + \alpha)]_i, \quad \forall \alpha \in B_p(L),$$

where $B_p(L_{\text{cons}})$ represents the p -norm ball of radius L_{cons} , that restricts the perturbation size to $\|\alpha\|_p \leq L_{\text{cons}}$. We also call L_{cons} as the construction bound.

Recently, Differential Privacy (DP) has emerged as a promising approach to enhance model robustness. Originally developed to protect individual data in statistical databases, DP ensures that the output of an algorithm does not significantly change when a single individual's data is added or removed. This is typically achieved by injecting carefully calibrated randomness into the algorithm's computation. This property of prediction stability forms the foundation of the connection between DP and adversarial robustness, as explored in (Lecuyer et al., 2019). By design, models trained with DP noise are inherently less sensitive to small input perturbations, thereby improving their resistance to adversarial attacks.

Formally, given a model f which is (ε, δ) differentially private under a p -norm metric, it is guaranteed to be robust against adversarial perturbations α of size $\|\alpha\|_p \leq 1$ if the following condition holds (Lecuyer et al., 2019):

$$E([f(x)]_k) > e^{2\varepsilon} \max_{i:i \neq k} E([f(x)]_i) + (1 + e^\varepsilon)\delta, \exists k \in K,$$

where $E([f(x)]_k)$ is the expected confidence score for the correct label k , and $E([f(x)]_i)$ is the expected confidence score for other labels.

This condition certifies that any input satisfying the inequality is immune to adversarial attacks within the defined perturbation size. A stronger DP guarantee, meaning smaller values for ε and δ , expands the set of inputs for which this robustness holds. In this work, our goal is to explore how quantum noise can amplify the DP guarantee, thereby significantly enhancing the model's overall robustness.

B. Technical Proofs

In this section, we provide detailed proofs of the main theoretical results.

B.1. Proof of Theorem 4.1 and Supporting Lemmas

We investigate how the failure probability is amplified under quantum post-processing, assuming a fixed privacy loss parameter ε . Specifically, we aim to upper bound the quantity:

$$\sup_{x,x'} D_{e^\varepsilon} \left(Q^{(\eta)} \circ A(x) \parallel Q^{(\eta)} \circ A(x') \right) \quad (1)$$

Lemma B.1. *Let μ and ν be probability distributions such that $D_{e^\varepsilon}(\mu\|\nu) \leq \delta$, and define $\theta = D_{e^\varepsilon}(\mu\|\nu)$. Then, there exist distributions μ' , ν' , and ω , along with a parameter $\tilde{\varepsilon} := \log(1 + \frac{e^\varepsilon - 1}{\theta})$ such that:*

$$\mu = (1 - \theta)\omega + \theta\mu', \quad \nu = \frac{1 - \theta}{e^\varepsilon}\omega + \left(1 - \frac{1 - \theta}{e^\varepsilon}\right)\nu',$$

with disjoint distributions: $\mu' \perp \nu'$. Then, the following bound holds:

$$D_{e^\varepsilon}(\mu\|\nu) = \theta \cdot D_{e^\varepsilon}(\mu'\|\nu')$$

Proof. Studied in (Balle et al., 2019a) □

Let the output distributions of A be denoted by $\mu = A(x)$ and $\nu = A(x')$, where $\mu, \nu \in \mathcal{P}(\mathbb{Y})$. Lemma B.1, originally studied in (Balle et al., 2019a), establishes a decomposition of two distributions μ and ν based on their divergence $\theta = D_{e^\varepsilon}(\mu\|\nu)$. Specifically, μ is decomposed into a mixture of an overlapping component ω and a residual component μ' , while ν is similarly decomposed into ω and a residual ν' . The shared component ω is defined via the density $p_\omega = \frac{\min(p_\mu, e^\varepsilon p_\nu)}{1 - \theta}$. The remaining distributions μ' and ν' correspond to the non-overlapping parts of μ and ν , and it is shown that they have disjoint support (i.e., $\mu' \perp \nu'$). Lemma B.1 also yields a transformation of the divergence between μ and ν in terms of the divergence between their respective components μ' and ν' , specifically $D_{e^\varepsilon}(\mu\|\nu) = \theta \cdot D_{e^\varepsilon}(\mu'\|\nu')$. Because the quantum process Q is a linear map (Nielsen & Chuang, 2010), it preserves convex combinations of input distributions. Consequently, we obtain

$$D_{e^\varepsilon}(\mu Q\|\nu Q) = \theta \cdot D_{e^\varepsilon}(\mu' Q\|\nu' Q) \quad (2)$$

In addition, the orthogonality of μ' and ν' plays a crucial role in analyzing the contraction behavior of post-processing mechanisms, as will be demonstrated in the following lemma.

Lemma B.2. *Given a post-process mechanism Q , we have:*

$$\sup_{\mu \perp \nu} D_\varepsilon(\mu Q\|\nu Q) \leq \sup_{y \neq y'} D_\varepsilon(Q(y)\|Q(y'))$$

Proof. Studied in (Balle et al., 2019a) □

Lemma B.2 establishes an upper bound on the divergence between two orthogonal distributions after applying a post-processing mechanism. Let τ_y denote the point mass distribution at y , i.e., $\tau_y(\tilde{y}) = 1$ if $\tilde{y} = y$ and $\tau_y(\tilde{y}) = 0$ otherwise. Then, $\mu = \sum_{y \in \text{supp}(\mu)} \mu(y) \tau_y$ and similarly for ν . By convexity of D_{e^ε} and linearity of Q , we have:

$$D_{e^\varepsilon}(\mu Q \| \nu Q) \leq \sup_{y \neq y'} D_{e^\varepsilon}(\tau_y Q \| \tau_{y'} Q) \leq \sup_{y \neq y'} D_{e^\varepsilon}(Q(y) \| Q(y'))$$

Together, Lemmas B.1 and B.2 clarify how the divergence between the outputs of A transforms under post-processing. It remains to analyze the divergence induced solely by $Q^{(\eta)}$, allowing us to focus on bounding:

$$\sup_{y \neq y'} D_{e^\varepsilon}(Q^{(\eta)}(y) \| Q^{(\eta)}(y')) \tag{3}$$

Lemma B.3. *Given a measurement $E = \{E_i\}$ with $\sum_i E_i = I$, and two quantum states ρ and ρ' , the classical hockey-stick divergence of the resulting probability distributions is less than or equal to the quantum hockey-stick divergence between the states.*

$$D_\alpha(P \| P') \leq D_\alpha^{(q)}(\rho \| \rho')$$

Proof. The quantum hockey-stick divergence is defined as:

$$D_\alpha^{(q)}(\rho \| \rho') = \text{Tr}[(\rho - \alpha\rho')_+],$$

where A_+ denotes the positive part of a Hermitian operator A . Let us define the operator $A = \rho - \alpha\rho'$.

Applying measurement E to ρ and ρ' yields probability distributions with elements:

$$P(i) = \text{Tr}(E_i \rho), \quad P'(i) = \text{Tr}(E_i \rho').$$

The classical hockey-stick divergence is defined as:

$$D_\alpha(P \| P') = \sum_i [P(i) - \alpha P'(i)]_+,$$

where $[x]_+ = \max(x, 0)$.

We begin the proof from the definition of the classical divergence:

$$\begin{aligned} D_\alpha(P \| P') &= \sum_i \max(0, \text{Tr}(E_i \rho) - \alpha \text{Tr}(E_i \rho')) \\ &= \sum_i \max(0, \text{Tr}(E_i(\rho - \alpha\rho'))) \\ &= \sum_i \max(0, \text{Tr}(E_i A)) \end{aligned}$$

For any positive semi-definite operator E_i and any Hermitian operator A , it holds that $\text{Tr}(E_i A) \leq \text{Tr}(E_i A_+)$. Since A_+ is a positive semi-definite operator, $\text{Tr}(E_i A_+)$ is non-negative. Therefore, we can conclude that $\max(0, \text{Tr}(E_i A)) \leq \text{Tr}(E_i A_+)$.

Applying this inequality to our expression, we get:

$$\begin{aligned}
 D_\alpha(P \parallel P') &\leq \sum_i \text{Tr}(E_i A_+) \\
 &= \text{Tr}\left(\sum_i E_i A_+\right) \\
 &= \text{Tr}\left(\left(\sum_i E_i\right) A_+\right) \\
 &= \text{Tr}(I \cdot A_+) \\
 &= D_\alpha^{(q)}(\rho \parallel \rho').
 \end{aligned}$$

□

Lemma B.3 establishes the dependence between classical and quantum hockey-stick divergences under a fixed measurement. As a consequence, we can eliminate the explicit measurement map f_{mea} from the post-processing pipeline. Specifically, we have:

$$D_\alpha(Q^{(\eta)}(y) \parallel Q^{(\eta)}(y')) \leq D_\alpha^{(q)}(f_{\text{dep}}^{(\eta)} \circ f_{\text{enc}}(y) \parallel f_{\text{dep}}^{(\eta)} \circ f_{\text{enc}}(y')) \quad (4)$$

Lemma B.4. *Given a depolarizing channel $f_{\text{dep}}^{(\eta)}(\rho) = \eta \frac{I}{d} + (1 - \eta)\rho$, for $\eta \in [0, 1]$ and $\alpha \geq 1$, we have:*

$$D_\alpha^{(q)}(f_{\text{dep}}^{(\eta)}(\rho) \parallel f_{\text{dep}}^{(\eta)}(\rho')) \leq \max\left\{0, (1 - \alpha)\frac{\eta}{d} + (1 - \eta)D_\alpha^{(q)}(\rho \parallel \rho')\right\}$$

Proof. Define the operator:

$$U = f_{\text{dep}}^{(\eta)}(\rho) - \alpha f_{\text{dep}}^{(\eta)}(\rho) = (1 - \eta)(\rho - \alpha\rho') + \eta(1 - \alpha)\frac{I}{d}.$$

Then:

$$D_\alpha^{(q)}(f_{\text{dep}}^{(\eta)}(\rho) \parallel f_{\text{dep}}^{(\eta)}(\rho')) = \text{Tr}[U_+],$$

where U_+ denotes the positive part of U .

Let P_+ be the projector onto the positive eigenspace of U . Since $D_\alpha^{(q)}(f_{\text{dep}}^{(\eta)}(\rho) \parallel f_{\text{dep}}^{(\eta)}(\rho') > 0$, we have $\text{Tr}[P_+] \geq 1$. Then:

$$\begin{aligned}
 \text{Tr}[U_+] &= \text{Tr}[P_+ U] \\
 &= (1 - \eta)\text{Tr}[P_+(\rho - \alpha\rho')] + (1 - \alpha)\frac{\eta}{d}\text{Tr}[P_+] \\
 &\leq (1 - \eta)D_\alpha^{(q)}(\rho \parallel \rho') + (1 - \alpha)\frac{\eta}{d},
 \end{aligned}$$

since $\text{Tr}[P_+] \geq 1$ and $1 - \alpha \leq 0$.

□

Lemma B.4 establishes that the quantum hockey-stick divergence contracts under a depolarizing channel by a factor of $(1 - \eta)$, with an additive term depending on α and the dimension d . Applying this result with $\rho = f_{\text{enc}}(y)$ and $\rho' = f_{\text{enc}}(y')$ yields an upper bound on the right-hand side of Equation 4, which in turn provides a bound for Equation 3.

Theorem 4.1 (Amplification on Failure Probability). *Let $A : \mathbb{X} \rightarrow \mathcal{P}(\mathbb{Y})$ be a classical mechanism satisfying (ε, δ) -DP where $A = f_{\text{par}} \circ f_{\text{cdp}}$, and let $Q^{(\eta)} : \mathbb{Y} \rightarrow \mathcal{P}(\mathbb{Z})$ be a quantum mechanism in a d -dimensional Hilbert space defined as $Q^{(\eta)} = f_{\text{mea}} \circ f_{\text{dep}}^{(\eta)} \circ f_{\text{enc}}$ where $0 \leq \eta \leq 1$ is the depolarizing noise factor. Then, the composed mechanism $Q^{(\eta)} \circ A$ satisfies (ε', δ') -DP, where*

$$\varepsilon' = \varepsilon, \quad \delta' = \left[\frac{\eta(1 - e^\varepsilon)}{d} + (1 - \eta)\delta \right]_+$$

Proof. Let $\mu = A(x)$ and $\nu = A(x')$ be the output distributions of the mechanism A on neighboring inputs x and x' . We aim to bound the hockey-stick divergence

$$D_{e^\varepsilon}(\mu Q^{(\eta)} \| \nu Q^{(\eta)}).$$

By Lemma B.1, we can decompose μ and ν using a parameter $\theta = D_{e^\varepsilon}(\mu \| \nu)$ and define auxiliary distributions μ' , ν' , and ω with $\mu' \perp \nu'$ such that

$$\mu = (1 - \theta)\omega + \theta\mu', \quad \nu = \frac{1 - \theta}{e^\varepsilon}\omega + \left(1 - \frac{1 - \theta}{e^\varepsilon}\right)\nu'.$$

Additionally, define $\tilde{\varepsilon} = \log(1 + \frac{e^\varepsilon - 1}{\theta})$. By Lemma B.1, it follows that

$$D_{e^\varepsilon}(\mu \| \nu) \leq \theta \cdot D_{e^{\tilde{\varepsilon}}}(\mu' \| \nu').$$

We now consider the post-processed outputs:

$$\begin{aligned} & D_{e^\varepsilon}(\mu Q^{(\eta)} \| \nu Q^{(\eta)}) \\ & \leq \theta \cdot D_{e^{\tilde{\varepsilon}}}(\mu' Q^{(\eta)} \| \nu' Q^{(\eta)}) \\ & \leq \theta \cdot \sup_{y \neq y'} D_{e^{\tilde{\varepsilon}}}(Q^{(\eta)}(y) \| Q^{(\eta)}(y')) \text{ (Lemma B.2)} \\ & \leq \theta \cdot \sup_{y \neq y'} D_{e^{\tilde{\varepsilon}}}^{(q)}(f_{\text{dep}}^{(\eta)} \circ f_{\text{enc}}(y) \| f_{\text{dep}}^{(\eta)} \circ f_{\text{enc}}(y')) \text{ (Lemma B.3)} \\ & = \theta \cdot \sup_{\rho, \rho'} D_{e^{\tilde{\varepsilon}}}^{(q)}(f_{\text{dep}}^{(\eta)}(\rho) \| f_{\text{dep}}^{(\eta)}(\rho')) \\ & \leq \theta \cdot \max \left\{ 0, \frac{\eta(1 - e^{\tilde{\varepsilon}})}{d} + (1 - \eta) \cdot D_{e^{\tilde{\varepsilon}}}^{(q)}(\rho \| \rho') \right\} \text{ (Lemma B.4)} \\ & \leq \max \left\{ 0, \frac{\theta\eta(1 - e^{\tilde{\varepsilon}})}{d} + \theta(1 - \eta) \right\} \text{ (Because } D_{e^{\tilde{\varepsilon}}}^{(q)}(\rho \| \rho') \leq 1) \end{aligned}$$

Recall that $e^{\tilde{\varepsilon}} = 1 + \frac{e^\varepsilon - 1}{\theta}$, we substitute this into the expression:

$$\begin{aligned} \frac{\theta\eta(1 - e^{\tilde{\varepsilon}})}{d} &= \frac{\theta\eta}{d} \left(1 - \left(1 + \frac{e^\varepsilon - 1}{\theta} \right) \right) \\ &= \frac{\theta\eta}{d} \left(-\frac{e^\varepsilon - 1}{\theta} \right) \\ &= \frac{\eta(1 - e^\varepsilon)}{d} \end{aligned}$$

Additionally, since the original mechanism A is (ε, δ) -DP, we have $\theta = D_{e^\varepsilon}(\mu \| \nu) \leq \delta$. Because $1 - \eta \geq 0$, we have the final result:

$$D_{e^\varepsilon}(\mu Q^{(\eta)} \| \nu Q^{(\eta)}) \leq \left[\frac{\eta(1 - e^\varepsilon)}{d} + (1 - \eta)\delta \right]_+$$

□

Theorem 4.1 establishes a bound on the failure probability δ' of the composed mechanism $Q^{(\eta)} \circ A$, while keeping the privacy loss fixed at $\varepsilon' = \varepsilon$. This result is derived by sequentially applying Lemmas B.2, B.3, and B.4 to Equation 2. From the final bound, it follows that for $\varepsilon \in [0, 1]$, we have $\delta' \leq \delta$. Therefore, the failure probability is strictly reduced, resulting in a privacy amplification effect, as formally stated in Corollary 4.2.

Based on (Lecuyer et al., 2019), we derive an explicit condition for certifiable adversarial robustness of the composed mechanism $Q^{(\eta)} \circ A$ in Corollary 4.3. This condition defines a robustness threshold that the model's expected confidence scores must exceed. Notably, due to the privacy amplification effect formalized in Corollary 4.2, the robustness threshold under the composed mechanism (parameterized by δ') is strictly lower than that of the original classical mechanism (parameterized by δ). As a result, quantum post-processing provably enlarges the set of inputs for which adversarial robustness can be guaranteed. For further details on adversarial robustness, we refer readers to Appendix A.

Corollary 4.2. *The composed mechanism $Q^{(\eta)} \circ A$ satisfies (ε, δ') -DP with $\delta' < \delta$, thus strictly amplifying the overall failure probability.*

Proof. The goal is to show that $\delta' < \delta$ for any non-trivial case where quantum post-processing is active ($\eta > 0$). From Theorem 4.1, we have:

$$\delta' = \left[\frac{\eta(1 - e^\varepsilon)}{d} + (1 - \eta)\delta \right]_+$$

Let the first term be $C = \frac{\eta(1 - e^\varepsilon)}{d}$. Since $\eta > 0$, $d \geq 2$, and $\varepsilon > 0$, we have $C \leq 0$. Since C is strictly negative, $C + (1 - \eta)\delta < (1 - \eta)\delta \leq \delta$. Thus, $\delta' < \delta$. \square

Corollary 4.3. *The composed mechanism $C = Q^{(\eta)} \circ A$ is certifiably robust against adversarial perturbations for an input $x \in \mathbb{X}$ if the following condition holds for the correct class k :*

$$\mathbb{E}[[C(x)]_k] > e^{2\varepsilon} \max_{i \neq k} \mathbb{E}[[C(x)]_i] + (1 + e^\varepsilon)\delta'$$

Proof. Studied in (Lecuyer et al., 2019). \square

B.2. Proof of Theorem 4.4 and Supporting Lemmas

We investigate how the composed mechanism $Q^{(\eta)} \circ A$ can simultaneously amplify both the privacy loss ε and the failure probability δ . Our approach relies on the *Advanced Joint Convexity* theory, originally introduced in (Balle et al., 2018). We restate the theory below as Lemma B.5.

Lemma B.5 (Advanced Joint Convexity). *Let μ, μ' be probability distributions such that*

$$\mu = (1 - \sigma)\mu_0 + \sigma\mu_1, \quad \mu' = (1 - \sigma)\mu_0 + \sigma\mu'_1,$$

for some $\sigma \in [0, 1]$, and distributions μ_0, μ_1, μ'_1 . Given $\alpha \geq 1$, define $\alpha' = 1 + \sigma(\alpha - 1)$, $\beta = \frac{\alpha'}{\alpha}$. Then the following inequality holds:

$$D_{\alpha'}(\mu\|\mu') \leq (1 - \beta)\sigma D_\alpha(\mu_1\|\mu_0) + \beta\sigma D_\alpha(\mu_1\|\mu'_1)$$

Proof. Studied in (Balle et al., 2018) \square

Lemma B.5 provides an upper bound on the divergence $D_{\alpha'}(\mu\|\mu')$ in terms of D_α divergences between the component distributions μ_0, μ_1 , and μ'_1 . The bound becomes tighter as the contribution of the shared (overlapping) distribution μ_0 , controlled by the mixing parameter σ , increases. Returning to our analysis, given $\mu = A(x)$ and $\nu = A(x')$ for adjacent inputs $x \sim x'$, and a tighter privacy loss $\varepsilon' = \log[1 + \sigma(e^\varepsilon - 1)]$ we are able to bound $D_{e^{\varepsilon'}}(\mu Q^{(\eta)}\|\nu Q^{(\eta)})$ by identifying the shared component between the distributions $\mu Q^{(\eta)}$ and $\nu Q^{(\eta)}$ as illustrated in Lemma B.6.

Lemma B.6. *Let ρ be a density matrix on a d -dimensional Hilbert space, and let*

$$\rho' = f_{dep}(\rho) = \eta \frac{I}{d} + (1 - \eta)\rho$$

be its depolarized version, where $0 \leq \eta \leq 1$. Let $\{E_k\}_{k=1}^K$ be a POVM satisfying $\sum_k E_k = I$. Then, the measurement probabilities satisfy:

$$\zeta'(k) = \frac{\eta}{d} \text{Tr}(E_k) + (1 - \eta)\zeta(k),$$

where $\zeta' = f_{mea}(\rho')$ and $\zeta = f_{mea}(\rho)$ with $\zeta', \zeta \in \mathcal{P}(\mathbb{Z})$.

Proof. By linearity of the trace operator,

$$\begin{aligned}
 \zeta'(k) &= \text{Tr}(E_k \rho') \\
 &= \text{Tr} \left(E_k \left(\eta \frac{I}{d} + (1 - \eta) \rho \right) \right) \\
 &= \eta \text{Tr} \left(E_k \frac{I}{d} \right) + (1 - \eta) \text{Tr}(E_k \rho) \\
 &= \frac{\eta}{d} \text{Tr}(E_k) + (1 - \eta) \zeta_k.
 \end{aligned}$$

□

Lemma B.6 establishes how depolarizing noise in the quantum system \mathcal{H} affects the resulting classical output distribution over \mathbb{Z} . Specifically, it shows that the measurement distribution under depolarization becomes a convex combination of the original (noiseless) distribution and that of a maximally mixed state, with the noise strength η controlling the mixing ratio.

Based on Lemma B.6, we can decompose the output distributions $\mu Q^{(\eta)}$ and $\nu Q^{(\eta)}$ accordingly. By definition, the quantum mechanism $Q^{(\eta)}$ can be expressed as a convex combination of two mechanisms: $Q^{(0)}$ (applies no noise) and $Q^{(1)}$ (applies full depolarizing noise). The mechanism $Q^{(1)}$ is constant, as it always outputs the measurement distribution of a maximally mixed state. That is, for all $y \in \mathbb{Y}$, we have $Q^{(1)}(y)(k) = \frac{\text{Tr}(E_k)}{d}$, where E_k is the k -th POVM element and $d = \dim(\mathcal{H})$. We denote this constant output distribution as ζ_{mix} . On the other hand, $Q^{(0)}(y)$ corresponds to the noiseless distribution ζ , and $Q^{(\eta)}(y)$ corresponds to the distribution ζ' defined in Lemma B.6. Using the decomposition given by the lemma, we have

$$Q^{(\eta)}(y) = \eta Q^{(1)}(y) + (1 - \eta) Q^{(0)}(y), \quad \forall y \in \mathbb{Y}$$

Using the linearity of $Q^{(\eta)}$ and the representations $\mu = \sum_{y \in \text{supp}(\mu)} \mu(y) \tau_y$ and $\nu = \sum_{y \in \text{supp}(\nu)} \nu(y) \tau_y$, we obtain $\mu Q^{(\eta)} = \eta \zeta_{\text{mix}} + (1 - \eta) \mu Q^{(0)}$, and $\nu Q^{(\eta)} = \eta \zeta_{\text{mix}} + (1 - \eta) \nu Q^{(0)}$.

By applying the *Advanced Joint Convexity* theory (Lemma B.5) on $\mu Q^{(\eta)}$ and $\nu Q^{(\eta)}$ with $\varepsilon' = \log(1 + (1 - \eta)(e^\varepsilon - 1))$ and $\beta = e^{\varepsilon' - \varepsilon}$, we have:

$$D_{e^{\varepsilon'}}(\mu Q^{(\eta)} || \nu Q^{(\eta)}) \leq (1 - \eta) \left((1 - \beta) D_{e^\varepsilon}(\mu Q^{(0)} || \zeta_{\text{mix}}) + \beta D_{e^\varepsilon}(\mu Q^{(0)} || \nu Q^{(0)}) \right) \quad (5)$$

Lemma B.7. *Given the measurement distribution of a maximally mixed state ζ_{mix} and an arbitrary distribution $z \in \mathcal{P}(\mathbb{Z})$, we have:*

$$D_\alpha(z || \zeta_{\text{mix}}) \leq 1 - \alpha \min_k \left(\frac{\text{Tr}(E_k)}{d} \right)$$

Proof. Recall the definition of the hockey-stick divergence:

$$D_\alpha(z || \zeta_{\text{mix}}) = \sum_k [z(k) - \alpha \zeta_{\text{mix}}(k)]_+,$$

where $[x]_+ = \max\{x, 0\}$. Since $\zeta_{\text{mix}}(k) = \frac{\text{Tr}(E_k)}{d} \geq \varphi = \min_k \left(\frac{\text{Tr}(E_k)}{d} \right)$, we have

$$[z(k) - \alpha \zeta_{\text{mix}}(k)]_+ \leq [z(k) - \alpha \varphi]_+.$$

Summing over k yields

$$D_\alpha(z || \zeta_{\text{mix}}) \leq \sum_k [z(k) - \alpha \varphi]_+.$$

Since $\sum_k z(k) = 1$, it follows that

$$\sum_k [z(k) - \alpha \varphi]_+ \leq 1 - \alpha \varphi.$$

Therefore,

$$D_\alpha(z\|\zeta_{\text{mix}}) \leq 1 - \alpha \min_k \left(\frac{\text{Tr}(E_k)}{d} \right).$$

□

Based on Lemma B.7, we can derive an upper bound on $D_{e^\varepsilon}(\mu Q^{(0)}\|\zeta_{\text{mix}})$ in terms of the trace values of the POVM elements. Additionally, from the data-processing inequality for the hockey-stick divergence, we have $D_{e^\varepsilon}(\mu Q^{(0)}\|\nu Q^{(0)}) \leq D_{e^\varepsilon}(\mu\|\nu) \leq \delta$. Combining these results, we obtain an improved bound for Equation 5:

$$D_{e^{\varepsilon'}}(\mu Q^{(\eta)}\|\nu Q^{(\eta)}) \leq (1 - \eta) \left(1 - e^{\varepsilon' - \varepsilon}(1 - \delta) - (e^\varepsilon - e^{\varepsilon'})\varphi \right)$$

, where $\varphi = \min_k \left(\frac{\text{Tr}(E_k)}{d} \right)$. This result is formalized in Theorem 4.4, which characterizes how depolarizing noise amplifies the privacy guarantees of the composed mechanism $Q^{(\eta)} \circ A$. Specifically, the mechanism satisfies (ε', δ') -DP, where $\varepsilon' = \log(1 + (1 - \eta)(e^\varepsilon - 1))$ and $\delta' = (1 - \eta) \left[1 - e^{\varepsilon' - \varepsilon}(1 - \delta) - (e^\varepsilon - e^{\varepsilon'})\varphi \right]$.

Theorem 4.4 reveals that the amplified failure probability δ' depends on the choice of POVMs. In particular, δ' becomes tighter as $\varphi = \min_k \left(\frac{\text{Tr}(E_k)}{d} \right)$ increases. This insight leads to Corollary 4.5, highlighting that δ' is minimized when all POVM elements E_k have equal trace (i.e., $\text{Tr}(E_k) = \frac{1}{K}$).

Contrarily, $\varepsilon' \leq \varepsilon$ for all $\eta \in [0, 1]$, the privacy loss in terms of ε is always reduced. However, the bound on δ is only improved (i.e., $\delta' \leq \delta$) when the noise level η exceeds the threshold given in Corollary 4.6. This condition highlights that a sufficient level of quantum noise is required to achieve strict amplification of the privacy guarantee in both parameters.

Theorem 4.4 (Amplification on Privacy Loss). *Let $A = f_{\text{par}} \circ f_{\text{cdp}}$ be (ε, δ) -DP, and $Q^{(\eta)} = f_{\text{mea}} \circ f_{\text{dep}}^{(\eta)} \circ f_{\text{enc}}$ be a quantum mechanism in a d -dimensional Hilbert space where $0 \leq \eta \leq 1$ is the depolarizing noise factor. Then, the composition $Q^{(\eta)} \circ A$ is (ε', δ') -DP where $\varepsilon' = \log(1 + (1 - \eta)(e^\varepsilon - 1))$ and $\delta' = (1 - \eta) \left(1 - e^{\varepsilon' - \varepsilon}(1 - \delta) - (e^\varepsilon - e^{\varepsilon'})\varphi \right)$ with $\varphi = \min_k \left(\frac{\text{Tr}(E_k)}{d} \right)$.*

Proof. Let $x, x' \in \mathbb{X}$ be neighboring inputs, i.e., $x \simeq x'$. Let $\mu = A(x)$ and $\nu = A(x')$ denote the output distributions of A . From the definition, we have $Q^{(0)}$ and $Q^{(1)}$ which are the mechanisms without noise and with full noise. We can see that $Q^{(1)}$ is a constant mechanism because the output of $Q^{(1)}$ is always the measurement of a maximally mixed state, i.e., $Q^{(1)}(y)(k) = \frac{\text{Tr}(E_k)}{d}$ with $\forall y \in \mathbb{Y}$. Based on Lemma B.6, we have:

$$Q^{(\eta)}(y) = \eta Q^{(1)}(y) + (1 - \eta)Q^{(0)}(y), \forall y \in \mathbb{Y}$$

. Thus, we can write $Q^{(\eta)}$ as a mixture of $Q^{(0)}$ and $Q^{(1)}$ where $Q^{(\eta)} = \eta Q^{(1)} + (1 - \eta)Q^{(0)}$.

Let the constant output of $Q^{(1)}$ be ζ_{mix} . Based on the advanced joint convexity theorem in (Balle et al., 2018), given $\varepsilon' = \log(1 + (1 - \eta)(e^\varepsilon - 1))$, we have:

$$\begin{aligned} & D_{e^{\varepsilon'}}(\mu Q^{(\eta)}\|\nu Q^{(\eta)}) \\ &= D_{e^{\varepsilon'}}(\eta\mu Q^{(1)} + (1 - \eta)\mu Q^{(0)}\|\eta\nu Q^{(1)} + (1 - \eta)\nu Q^{(0)}) \\ &= D_{e^{\varepsilon'}}(\eta\zeta_{\text{mix}} + (1 - \eta)\mu Q^{(0)}\|\eta\zeta_{\text{mix}} + (1 - \eta)\nu Q^{(0)}) \\ &= (1 - \eta)D_{e^\varepsilon}(\mu Q^{(0)}\|(1 - \beta)\zeta_{\text{mix}} + \beta\nu Q^{(0)}) \\ &\quad (\text{Based on the advanced joint convexity theorem, } \beta = e^{\varepsilon' - \varepsilon}) \\ &\leq (1 - \eta) \left((1 - \beta)D_{e^\varepsilon}(\mu Q^{(0)}\|\zeta_{\text{mix}}) + \beta D_{e^\varepsilon}(\mu Q^{(0)}\|\nu Q^{(0)}) \right) \end{aligned}$$

We have $D_{e^\varepsilon}(\mu Q^{(0)}\|\zeta_{\text{mix}}) \leq 1 - e^\varepsilon \min_k \left(\frac{\text{Tr}(E_k)}{d} \right) = 1 - e^\varepsilon \varphi$ and $D_{e^\varepsilon}(\mu Q^{(0)}\|\nu Q^{(0)}) \leq D_{e^\varepsilon}(\mu\|\nu) \leq \delta$. Thus, we can conclude:

$$D_{e^{\varepsilon'}}(\mu Q^{(\eta)}\|\nu Q^{(\eta)}) \leq (1 - \eta) \left(1 - e^{\varepsilon' - \varepsilon}(1 - \delta) - (e^\varepsilon - e^{\varepsilon'})\varphi \right)$$

□

Corollary 4.5. Let $\{E_k\}_{k=1}^K$ be the POVM used in f_{mea} . Then, the amplified failure probability δ' in Theorem 4.4 is minimized when all POVM elements have equal trace (i.e., $\text{Tr}[E_k] = \frac{d}{K}$ for all $k \in \{1, \dots, K\}$).

Proof. The goal is to minimize the amplified failure probability δ' with respect to the choice of the POVM $\{E_k\}_{k=1}^K$. From Theorem 4.4, the expression for δ' is:

$$\delta' = (1 - \eta)(1 - e^{\varepsilon' - \varepsilon}(1 - \delta) - (e^\varepsilon - e^{\varepsilon'}))\varphi$$

All terms in this expression are independent of the specific measurement choice except for $\varphi = \min_k \left(\frac{\text{Tr}(E_k)}{d} \right)$.

To analyze how δ' depends on φ , we examine the sign of $-(1 - \eta)(e^\varepsilon - e^{\varepsilon'})$. Since $\eta \in [0, 1]$ and $\varepsilon' \leq \varepsilon$, this coefficient is non-positive. Thus, δ' is a monotonically decreasing function of φ .

Therefore, to minimize δ' , we must maximize φ . This is equivalent to maximizing $\min_k(\text{Tr}(E_k))$ subject to the POVM completeness constraint $\sum_{k=1}^K E_k = I$. Taking the trace of the completeness relation gives:

$$\sum_{k=1}^K \text{Tr}(E_k) = \text{Tr}(I) = d$$

The function $\min_k(\text{Tr}(E_k))$ is maximized when all $\text{Tr}[E_k]$ are equal. Thus, the optimal choice is to have $\text{Tr}[E_k] = d/K$ for all k . □

Corollary 4.6. Given an optimal measurement such that $\text{Tr}[E_k] = \frac{d}{K} \forall k$, the composed mechanism $Q^{(\eta)} \circ A$ strictly improves the privacy guarantee (i.e., $\varepsilon' \leq \varepsilon$ and $\delta' \leq \delta$) if

$$\eta \geq 1 - \frac{\delta}{(1 - \delta)(1 - e^{-\varepsilon}) - (e^\varepsilon - 1)/K}$$

Proof. We find the condition on η that ensures $\delta' \leq \delta$ under the assumption of an optimal measurement, where, from Corollary 4.5, we have $\varphi = 1/K$. The guarantee $\varepsilon' \leq \varepsilon$ holds for all $\eta \in [0, 1]$.

We start with the inequality $\delta' \leq \delta$ using the expression from Theorem 4.4:

$$(1 - \eta)(1 - e^{\varepsilon' - \varepsilon}(1 - \delta) - (e^\varepsilon - e^{\varepsilon'}))\varphi \leq \delta$$

Substitute the identities $e^{\varepsilon' - \varepsilon} = 1 - \eta + \eta e^{-\varepsilon}$, $e^\varepsilon - e^{\varepsilon'} = \eta(e^\varepsilon - 1)$, and $\varphi = 1/K$, we have:

$$(1 - \eta) \left(1 - (1 - \eta + \eta e^{-\varepsilon})(1 - \delta) - \frac{\eta(e^\varepsilon - 1)}{K} \right) \leq \delta$$

The expression inside the main brackets simplifies to $\delta + \eta(1 - \delta)(1 - e^{-\varepsilon}) - \frac{\eta(e^\varepsilon - 1)}{K}$. Substituting this back, expanding, and simplifying for $\eta > 0$, we have:

$$(1 - \delta)(1 - e^{-\varepsilon}) - \frac{e^\varepsilon - 1}{K} - \delta \leq \eta \left((1 - \delta)(1 - e^{-\varepsilon}) - \frac{e^\varepsilon - 1}{K} \right)$$

Solving for η gives the threshold:

$$\begin{aligned} \eta &\geq \frac{(1 - \delta)(1 - e^{-\varepsilon}) - (e^\varepsilon - 1)/K - \delta}{(1 - \delta)(1 - e^{-\varepsilon}) - (e^\varepsilon - 1)/K} \\ &= 1 - \frac{\delta}{(1 - \delta)(1 - e^{-\varepsilon}) - (e^\varepsilon - 1)/K} \end{aligned}$$

□

B.3. Proof of Theorem 4.10 and Supporting Lemmas

Here, we establish a rigorous framework to study the utility loss, defined as the absolute error between the noisy and noise-free versions of our mechanism. The final output of the mechanism is stochastic due to the sampling-based measurement process. Thus, we analyze the difference between the expected values of their output. The expected value represents the average behavior of a mechanism and provides a deterministic quantity that we can use to measure utility loss.

Formally, we define the expectation measurement function $f_{\text{exp}} : \mathcal{H} \rightarrow \mathbb{R}$ as:

$$f_{\text{exp}}(\rho) = \sum_k k \text{Tr}[E_k \rho] = \text{Tr} \left[\left(\sum_k k E_k \right) \rho \right] = \text{Tr}[E_{\text{exp}} \rho]$$

where $E_{\text{exp}} = \sum_k k E_k$ is the expectation value observable.

Using this function, we define our deterministic expectation mechanisms. The **full mechanism**, including classical and quantum noise, is $\mathcal{M}_{\text{full}}(x) = (f_{\text{exp}} \circ f_{\text{dep}}^{(\eta)} \circ f_{\text{enc}} \circ f_{\text{par}} \circ f_{\text{cdp}})(x)$. On the other hand, the **noise-free mechanism (clean)** is $\mathcal{M}_{\text{clean}}(x) = (f_{\text{exp}} \circ f_{\text{enc}} \circ f_{\text{par}})(x)$. The total utility loss is the worst-case absolute error between their expected outputs:

$$\text{Error} = \sup_{x \in \mathbb{X}} |\mathcal{M}_{\text{full}}(x) - \mathcal{M}_{\text{clean}}(x)|$$

To analyze this error, we introduce an **intermediate mechanism (half)** that includes only quantum noise as $\mathcal{M}_{\text{half}}(x) = (f_{\text{exp}} \circ f_{\text{dep}}^{(\eta)} \circ f_{\text{enc}} \circ f_{\text{par}})(x)$.

Lemma B.8. *The intermediate mechanism $\mathcal{M}_{\text{half}}$ is L_{∞} -Lipschitz with respect to the input perturbation κ , satisfying $|\mathcal{M}_{\text{half}}(x + \kappa) - \mathcal{M}_{\text{half}}(x)| \leq L_{\infty} \|\kappa\|_{\infty}$. L_{∞} is given by:*

$$L_{\infty} = 2(1 - \eta) \|E_{\text{exp}}\|_{\text{op}} \|W\|_{\infty} \left(\sum_j \|H_j\|_{\text{op}} \right)$$

Proof. First, we prove that a Lipschitz bound for a composition of functions can be obtained as the product of their individual Lipschitz constants. Specifically, suppose that f can be written as

$$f = f_1 \circ f_2 \circ \cdots \circ f_h,$$

where \circ denotes function composition, and each f_i admits a Lipschitz constant L_i for $i = 1, \dots, h$. Then, for any inputs x and a small deviation κ , it holds that

$$\begin{aligned} & \|f(x + \kappa) - f(x)\| \\ & \leq L_1 \|f_2 \circ \cdots \circ f_h(x + \kappa) - f_2 \circ \cdots \circ f_h(x)\| \\ & \leq L_1 L_2 \|f_3 \circ \cdots \circ f_h(x + \kappa) - f_3 \circ \cdots \circ f_h(x)\| \\ & \quad \vdots \\ & \leq \left(\prod_{i=1}^h L_i \right) \|\kappa\|. \end{aligned}$$

Since the mechanism $\mathcal{M}_{\text{half}}$ is expressed as a composition of f_{exp} , f_{dep}^{η} , f_{enc} , and f_{par} , our goal is to determine the Lipschitz bound for each individual function.

Lipschitz bound of f_{par} :

The function $f_{\text{par}} : \mathbb{X} \rightarrow \mathbb{Y}$ is defined as

$$f_{\text{par}}(x) = Wx + b,$$

‘Since b is a constant shift (which does not affect Lipschitz continuity), we have:

$$\|f_{\text{par}}(x + \kappa) - f_{\text{par}}(x)\| = \|W\kappa\| \leq \|W\|_{\infty} \|\kappa\|_{\infty},$$

Thus, f_{par} is $\|W\|_{\infty}$ -Lipschitz.

Lipschitz bound of f_{enc} :

The function $f_{\text{enc}} : \mathbb{Y} \rightarrow \mathcal{H}$ encodes a classical vector y into a density matrix $f_{\text{enc}}(y) = U_{\text{enc}}(y)|0\rangle\langle 0|U_{\text{enc}}(y)^\dagger$ where $U_{\text{enc}}(y) = \prod_{j=1}^N e^{-i(\mathbf{w}_j \cdot y_j + b_j)H_j}$. We need to bound the trace norm distance $f_{\text{enc}}(y + \kappa) - f_{\text{enc}}(y)$ in terms of $\|\kappa\|_{\infty}$.

$$\begin{aligned} & \|f_{\text{enc}}(y + \kappa) - f_{\text{enc}}(y)\| \\ &= \|U_{\text{enc}}(y + \kappa)\rho_0 U_{\text{enc}}(y + \kappa)^\dagger - U_{\text{enc}}(y)\rho_0 U_{\text{enc}}(y)^\dagger\| \\ &\leq 2\|U_{\text{enc}}(y + \kappa) - U_{\text{enc}}(y)\| \end{aligned}$$

where $\rho_0 = |0\rangle\langle 0|$ and we used the triangle inequality and properties of the trace norm. The difference between the unitary operators is bounded by:

$$\begin{aligned} & \|U_{\text{enc}}(y + \kappa) - U_{\text{enc}}(y)\| \\ &\leq \sum_{j=1}^N \|e^{-i(y_j + \kappa_j)H_j} - e^{-iy_jH_j}\| \\ &\leq \sum_{j=1}^N |\kappa_j| \|H_j\| \leq \sum_{j=1}^N \|H_j\| \|\kappa\|_{\infty} \end{aligned}$$

(Based on (Berberich et al., 2024))

Thus, f_{enc} is $2 \left(\sum_{j=1}^N \|H_j\| \right)$ -Lipschitz.

Lipschitz bound of $f_{\text{dep}}^{(\eta)}$:

The function $f_{\text{dep}}^{(\eta)} : \mathcal{H} \rightarrow \mathcal{H}$ models the depolarizing noise:

$$f_{\text{dep}}^{(\eta)}(\rho) = (1 - \eta)\rho + \eta \frac{I}{d},$$

where I is the identity matrix and d is the dimension of the Hilbert space.

Since the term $\eta \frac{I}{d}$ is constant, the difference between two outputs is:

$$\|f_{\text{dep}}^{(\eta)}(\rho) - f_{\text{dep}}^{(\eta)}(\sigma)\| = (1 - \eta)\|\rho - \sigma\|.$$

Thus, $f_{\text{dep}}^{(\eta)}$ is $(1 - \eta)$ -Lipschitz.

Lipschitz bound of f_{exp} :

The measurement function $f_{\text{mea}} : \mathcal{H} \rightarrow \mathbb{R}^K$, defined by a set of POVMs $\{E_k\}$, maps a quantum state ρ to a probability vector:

$$f_{\text{exp}}(\rho) = \sum_k k \text{Tr}(E_k \rho).$$

Given $E_{\text{exp}} = \sum_k kE_k$, by trace duality and Hölder’s inequality, we have:

$$\|f_{\text{exp}}(\rho) - f_{\text{exp}}(\rho')\| = |\text{Tr}(E_{\text{exp}}(\rho - \rho'))| \leq \|E_{\text{exp}}\|_{op} \|\rho - \rho'\|.$$

Therefore, f_{exp} is $\|E_{\text{exp}}\|_{op}$ -Lipschitz.

As a result, the mechanism $\mathcal{M}_{\text{half}}$ is L_∞ -Lipschitz where $L_\infty = 2(1 - \eta)\|E_{\text{exp}}\|_{\text{op}}\|W\|_\infty \left(\sum_j \|H_j\|_{\text{op}} \right)$.

□

Lemma B.8 establishes a bound on the sensitivity of $\mathcal{M}_{\text{half}}$ with respect to perturbations in its classical input. We use $\|\cdot\|_p$ to denote the p -norm, and $\|\cdot\|_{\text{op}}$ to denote the operator norm. The proof leverages the chain rule for Lipschitz continuity, where the overall Lipschitz constant L_∞ is given by the product of the individual constants associated with each component function in the composition, namely, f_{exp} , f_{dep} , f_{enc} , and f_{par} . In addition, we observe that if $\kappa \sim \mathcal{N}(0, \sigma^2 I)$, then $\mathcal{M}_{\text{half}}(x + \kappa)$ is equivalent in distribution to $\mathcal{M}_{\text{full}}(x)$. Thus, this lemma results in a bound on the difference between these two mechanisms.

Lemma B.9. *The absolute difference between the expected outputs of the intermediate and noise-free mechanisms is uniformly bounded by:*

$$|\mathcal{M}_{\text{half}}(x) - \mathcal{M}_{\text{clean}}(x)| \leq 2\eta\|E_{\text{exp}}\|_{\text{op}}$$

Proof. Let $\rho(x) = (f_{\text{enc}} \circ f_{\text{par}})(x)$ be the clean quantum state.

$$\begin{aligned} & |\mathcal{M}_{\text{half}}(x) - \mathcal{M}_{\text{clean}}(x)| \\ &= \left| \text{Tr}[f_{\text{exp}} \cdot f_{\text{dep}}^\eta(\rho(x))] - \text{Tr}(f_{\text{exp}} \cdot \rho(x)) \right| \\ &\leq \|E_{\text{exp}}\|_{\text{op}} \cdot \|f_{\text{dep}}^\eta(\rho(x)) - \rho(x)\| \quad (\text{Lipschitz property of } f_{\text{exp}}) \end{aligned}$$

The trace distance term is bounded as:

$$\|f_{\text{dep}}^\eta(\rho) - \rho\| = \|((1 - \eta)\rho + \eta \frac{I}{d}) - \rho\| = \eta \left\| \frac{I}{d} - \rho \right\|$$

Since ρ and I/d are both valid density matrices, the trace distance between them is at most 2. Thus, $\left\| \frac{I}{d} - \rho \right\| \leq 2$. Substituting this back gives the final bound of $2\eta\|E_{\text{exp}}\|_{\text{op}}$. □

Lemma B.9 directly bounds the difference between $\mathcal{M}_{\text{half}}$ and $\mathcal{M}_{\text{clean}}$. The proof leverages the Lipschitz property of the function f_{exp} and the fundamental property that the trace norm difference between any two density matrices is at most 2. Along with the result in Lemma B.8, we can establish the bound on the absolute error.

Theorem 4.10 (Utility Bound). *Let the classical noise be $\kappa \sim \mathcal{N}(0, \sigma^2 I)$ acting on an input space \mathbb{X} of dimension $d_X = \dim(\mathbb{X})$. For any desired failure probability $p > 0$, the utility loss is bounded probabilistically as:*

$$\Pr \left(\text{Error} \leq L_\infty \cdot \sigma \sqrt{2 \ln \frac{2d_X}{p}} + 2\eta\|E_{\text{exp}}\|_{\text{op}} \right) \geq 1 - p$$

where $L_\infty = 2(1 - \eta)\|E_{\text{exp}}\|_{\text{op}}\|W\|_\infty \left(\sum_j \|H_j\|_{\text{op}} \right)$.

Proof. We use the triangle inequality for the absolute error for a given x and classical noise κ :

$$\begin{aligned} & |\mathcal{M}_{\text{full}}(x) - \mathcal{M}_{\text{clean}}(x)| \\ &= |\mathcal{M}_{\text{half}}(x + \kappa) - \mathcal{M}_{\text{clean}}(x)| \\ &\leq |\mathcal{M}_{\text{half}}(x + \kappa) - \mathcal{M}_{\text{half}}(x)| + |\mathcal{M}_{\text{half}}(x) - \mathcal{M}_{\text{clean}}(x)| \end{aligned}$$

Applying our two lemmas, the first term is bounded by $L_\infty \cdot \|\kappa\|_\infty$ and the second term is bounded by $2\eta\|E_{\text{exp}}\|_{\text{op}}$.

$$\text{Error} \leq L_\infty \cdot \|\kappa\|_\infty + 2\eta\|E_{\text{exp}}\|_{\text{op}}$$

The stochastic error depends on the magnitude of $\|\kappa\|_\infty = \max_i |\kappa_i|$, where each component κ_i of the noise vector is an independent draw from a Gaussian distribution, $\kappa_i \sim \mathcal{N}(0, \sigma^2)$.

To obtain a high-probability bound on the maximum of d independent Gaussian variables, we can apply a standard union bound on their tails. For any desired failure probability $p > 0$, with probability at least $1 - p$, the infinity norm of κ is bounded by:

$$\|\kappa\|_\infty \leq \sigma \sqrt{2 \ln(2d_X/p)}$$

By combining these bounds, we can state that for any $p > 0$, the total utility loss is bounded with probability at least $1 - p$:

$$\text{Error} \leq L_\infty \cdot \sigma \sqrt{2 \ln \frac{2d_X}{p}} + 2\eta \|E_{\text{exp}}\|_{op}$$

□

Theorem 4.10 combines the previous results to provide a single utility guarantee. The proof exploits the triangle inequality to additively combine the bounds from Lemmas B.8 and B.9. As the classical noise is unbounded, the final guarantee is a high-probability statement showing the trade-off between utility loss and the classical (σ) and quantum (η) noise level.

B.4. Third Analysis — Extending to Other Quantum Noise Channels (extended)

In this section, beside delivering the proofs for Theorem 4.7 and 4.9, we provide more discussion on how the privacy amplification result of Theorem 4.1 can be extended to a broad class of quantum noise channels beyond depolarizing noise. First, we identify the essential mechanism responsible for privacy amplification. Then, we illustrate the generalization by analyzing two asymmetric and physically relevant noise processes: the Generalized Amplitude Damping (GAD) channel and the Generalized Dephasing (GD) channel.

B.4.1. KEY INSIGHT BEHIND THE GENERALIZATION

Here, first we review the proof trajectory of Theorem 4.1 presented in Appendix B.1. The analysis begins by decomposing the output distributions of the mechanism on neighboring inputs using Lemma B.1. It then reduces the divergence analysis to the worst-case pair of orthogonal inputs via Lemma B.2. Crucially, Lemma B.3 establishes that the classical hockey-stick divergence of the measurement outcomes is upper-bounded by the quantum hockey-stick divergence of the evolved quantum states.

We can see that in Theorem 4.1, the privacy amplification is derived from Lemma B.4, which establishes the contraction of the quantum hockey-stick divergence $D_\alpha^{(q)}$ under the depolarizing channel. While Theorem 4.1 utilizes the specific form of $D_{e^\epsilon}^{(q)}$, we discuss that even if we relax the bound to the standard trace distance $D_1^{(q)}$, the privacy guarantee still holds. Specifically, for any privacy parameter $\alpha \geq 1$ (where $\alpha = e^\epsilon$ in our context), the quantum hockey-stick divergence is upper-bounded by the trace distance divergence:

$$D_\alpha^{(q)}(\rho\|\sigma) = \text{Tr}[(\rho - \alpha\sigma)_+] \leq \text{Tr}[(\rho - \sigma)_+] = D_1^{(q)}(\rho\|\sigma).$$

This inequality holds because subtracting a larger multiple of σ (since $\alpha \geq 1$) reduces the positive part of the operator difference.

Then, the insight is that to generalize Theorem 4.1 to an arbitrary noise channel \mathcal{E} , we need to identify its contraction coefficient under the trace distance (or D_1 divergence). If a channel \mathcal{E} satisfies a contraction bound $\kappa(\mathcal{E})$ such that:

$$\sup_{\rho \neq \sigma} \frac{D_1(\mathcal{E}(\rho)\|\mathcal{E}(\sigma))}{D_1(\rho\|\sigma)} \leq \kappa(\mathcal{E}),$$

then the composed mechanism naturally satisfies a privacy amplification where the failure probability δ is scaled by $\kappa(\mathcal{E})$. In the following subsections, we apply this insight to two asymmetric noise channels.

B.4.2. GENERALIZED AMPLITUDE DAMPING CHANNEL (PROOF OF THEOREM 4.7)

Generalized Amplitude Damping (GAD) channel is a noise process describing energy exchange between a qubit and its thermal environment. Unlike depolarizing, GAD is inherently asymmetric because it drives the qubit toward a temperature-dependent equilibrium state while simultaneously suppressing quantum coherence. The channel is parameterized by a damping strength $\eta \in [0, 1]$ and an excitation probability $p \in [0, 1]$, where $p = 0$ corresponds to relaxation toward $|0\rangle$, $p = 1$ toward $|1\rangle$, and intermediate values represent nonzero-temperature behavior. This asymmetry makes GAD a realistic noise model for superconducting and trapped-ion devices. To formalize this, we consider the n -qubit channel acting on a single designated qubit:

$$f_{\text{GAD}}^{(p,\eta)} = I_{2^{n-1}} \otimes A_{\text{GAD}}^{(p,\eta)}.$$

Despite its non-unital nature, the GAD channel contracts distinguishability between quantum states. Differences in excitation probabilities shrink because all states relax toward the same thermal fixed point, while differences in coherence decay due to energy dissipation. In Lemma B.10, we construct the contraction coefficient of $f_{\text{GAD}}^{(p,\eta)}$.

Lemma B.10. *Let $A_{\text{GAD}}^{(p,\eta)}$ be the generalized amplitude damping (GAD) channel on a single qubit, with damping parameter $\eta \in [0, 1]$ and excitation parameter $p \in [0, 1]$. Define the n -qubit channel*

$$f_{\text{GAD}}^{(p,\eta)} := I_{2^{n-1}} \otimes A_{\text{GAD}}^{(p,\eta)},$$

Then the contraction coefficient of $f_{\text{GAD}}^{(p,\eta)}$ satisfies

$$\kappa(f_{\text{GAD}}^{(p,\eta)}) := \sup_{\rho \neq \sigma} \frac{D_1\left(f_{\text{GAD}}^{(p,\eta)}(\rho) \middle\| f_{\text{GAD}}^{(p,\eta)}(\sigma)\right)}{D_1(\rho \middle\| \sigma)} \leq 2\sqrt{\eta} - \eta$$

Proof. By definition $D_1(\rho \middle\| \sigma) = \frac{1}{2}\|\rho - \sigma\|_1$, so $\kappa(f_{\text{GAD}}^{(p,\eta)})$ is the trace-distance contraction coefficient of the channel $f_{\text{GAD}}^{(p,\eta)} = I_{2^{n-1}} \otimes A_{\text{GAD}}^{(p,\eta)}$:

$$\kappa(f_{\text{GAD}}^{(p,\eta)}) = \sup_{\rho \neq \sigma} \frac{\|f_{\text{GAD}}^{(p,\eta)}(\rho) - f_{\text{GAD}}^{(p,\eta)}(\sigma)\|_1}{\|\rho - \sigma\|_1}.$$

The supremum is over all n -qubit states ρ, σ , which may be entangled across the ancilla system and the noisy qubit.

Based on (Hirche, 2024), this is upper-bounded by the complete trace-distance contraction coefficient of the single-qubit channel $A_{\text{GAD}}^{(p,\eta)}$, defined as

$$\eta_{Tr}^c(A_{\text{GAD}}^{(p,\eta)}) := \sup_{k \geq 1} \sup_{\rho \neq \sigma} \frac{\|(I_k \otimes A_{\text{GAD}}^{(p,\eta)})(\rho) - (I_k \otimes A_{\text{GAD}}^{(p,\eta)})(\sigma)\|_1}{\|\rho - \sigma\|_1}.$$

Since $f_{\text{GAD}}^{(p,\eta)}$ is exactly $I_{2^{n-1}} \otimes A_{\text{GAD}}^{(p,\eta)}$ for one particular ancilla dimension, we have

$$\kappa(f_{\text{GAD}}^{(p,\eta)}) \leq \eta_{Tr}^c(A_{\text{GAD}}^{(p,\eta)}).$$

Based on the Lemma 9 and Proposition 28 in (Hirche, 2024), we have:

$$\begin{aligned} \kappa(f_{\text{GAD}}^{(p,\eta)}) &= \eta_{Tr}^c(A_{\text{GAD}}^{(p,\eta)}) \\ &\leq 1 - \alpha(A_{\text{GAD}}^{(p,\eta)}) \\ &= 1 - (1 - \sqrt{\eta})^2 \\ &= 1 - (1 - 2\sqrt{\eta} + \eta) \\ &= 2\sqrt{\eta} - \eta. \end{aligned}$$

□

Based on Lemma B.10, we now derive a privacy amplification result for the GAD channel in Theorem 4.7.

Theorem 4.7 (Amplification Under Generalized Amplitude Damping Noise). *Let $A : \mathbb{X} \rightarrow \mathcal{P}(\mathbb{Y})$ be a classical mechanism satisfying (ε, δ) -DP where $A = f_{\text{par}} \circ f_{\text{cdp}}$, and let $Q^{(p, \eta)} : \mathbb{Y} \rightarrow \mathcal{P}(\mathbb{Z})$ be a quantum mechanism in d -dimensional Hilbert space defined as $Q^{(p, \eta)} = f_{\text{mea}} \circ f_{\text{GAD}}^{(p, \eta)} \circ f_{\text{enc}}$. Then, the composed mechanism $Q^{(p, \eta)} \circ A$ satisfies (ε', δ') -DP, where*

$$\varepsilon' = \varepsilon, \quad \delta' = (2\sqrt{\eta} - \eta)\delta.$$

Proof. Let $\mu = A(x)$ and $\nu = A(x')$ be the output distributions of the mechanism A on neighboring inputs x and x' . We aim to bound the hockey-stick divergence

$$D_{e^\varepsilon}(\mu Q^{(p, \eta)} \| \nu Q^{(p, \eta)}).$$

By Lemma B.1, we can decompose μ and ν using a parameter $\theta = D_{e^\varepsilon}(\mu \| \nu)$ and define auxiliary distributions μ', ν' , and ω with $\mu' \perp \nu'$ such that

$$\mu = (1 - \theta)\omega + \theta\mu', \quad \nu = \frac{1 - \theta}{e^\varepsilon}\omega + \left(1 - \frac{1 - \theta}{e^\varepsilon}\right)\nu'.$$

Additionally, define $\tilde{\varepsilon} = \log\left(1 + \frac{e^\varepsilon - 1}{\theta}\right)$.

We now consider the post-processed outputs:

$$\begin{aligned} & D_{e^\varepsilon}(\mu Q^{(p, \eta)} \| \nu Q^{(p, \eta)}) \\ & \leq \theta \cdot D_{e^{\tilde{\varepsilon}}}(\mu' Q^{(p, \eta)} \| \nu' Q^{(p, \eta)}) && \text{(Lemma B.1)} \\ & \leq \theta \cdot \sup_{y \neq y'} D_{e^{\tilde{\varepsilon}}}(\mathbb{Q}^{(p, \eta)}(y) \| \mathbb{Q}^{(p, \eta)}(y')) && \text{(Lemma B.2)} \\ & \leq \theta \cdot \sup_{y \neq y'} D_{e^{\tilde{\varepsilon}}}^{(q)}\left(f_{\text{GAD}}^{(p, \eta)} \circ f_{\text{enc}}(y) \| f_{\text{GAD}}^{(p, \eta)} \circ f_{\text{enc}}(y')\right) && \text{(Lemma B.3)} \\ & = \theta \cdot \sup_{\rho, \rho'} D_{e^{\tilde{\varepsilon}}}^{(q)}\left(f_{\text{GAD}}^{(p, \eta)}(\rho) \| f_{\text{GAD}}^{(p, \eta)}(\rho')\right) && \text{(where } \rho, \rho' \text{ are pure)} \\ & \leq \theta \cdot \sup_{\rho, \rho'} D_1^{(q)}\left(f_{\text{GAD}}^{(p, \eta)}(\rho) \| f_{\text{GAD}}^{(p, \eta)}(\rho')\right) && (e^{\tilde{\varepsilon}} \geq 1) \\ & \leq \theta \cdot \sup_{\rho, \rho'} \left((2\sqrt{\eta} - \eta) \cdot D_1^{(q)}(\rho \| \rho')\right) && \text{(Lemma B.10)} \\ & \leq \theta \cdot (2\sqrt{\eta} - \eta) \cdot 1 && \text{(Because } D_{e^{\tilde{\varepsilon}}}^{(q)}(\rho \| \rho') \leq 1) \end{aligned}$$

Since the original mechanism A is (ε, δ) -DP, we have $\theta = D_{e^\varepsilon}(\mu \| \nu) \leq \delta$. We substitute this into the final bound:

$$D_{e^\varepsilon}(\mu Q^{(p, \eta)} \| \nu Q^{(p, \eta)}) \leq (2\sqrt{\eta} - \eta) \cdot \delta.$$

This yields the advertised DP parameters. \square

B.4.3. GENERALIZED DEPHASING CHANNEL (PROOF OF THEOREM 4.9)

Generalized Dephasing (GD) channel is one of the most fundamental and widely studied noise processes in quantum information. It suppresses quantum coherence while leaving classical populations unchanged. Specifically, this channel is formulated as:

$$A_{\text{GD}}^{(\eta)}(\rho) = (1 - \eta)\rho + \eta Z \rho Z$$

where $\eta \in [0, 1]$ is the dephasing parameter and Z is the Pauli-Z operator. From Proposition 33 in (Hirche, 2024), the complete trace-distance contraction coefficient of a single-qubit GD channel is exactly 1 (i.e., $\eta_{Tr}^c(A_{\text{GD}}^{(\eta)}) = 1$). This implies that no worst-case privacy amplification can be guaranteed under dephasing noise. In other words, for some input states, the noise does not reduce distinguishability at all. However, this worst case is only attained for states distinguished solely through diagonal differences. In many common QML architectures such as those using angle encoding, the encoded data occupies families of states where all information is carried in the off-diagonal components (coherences). In this setting, GD noise does provide nontrivial contraction, and thus we obtain privacy amplification. One instance of this setting is formally presented in Assumption 4.8.

Assumption 4.8 (Product Equatorial Encoding on All Qubits). *For each input $y \in \mathbb{Y}$, the encoder prepares a product state*

$$\rho_y = f_{\text{enc}}(y) = \bigotimes_{j=1}^n \rho_y^{(j)},$$

where each single-qubit factor $\rho_y^{(j)}$ is an equatorial state on the Bloch sphere, i.e.,

$$\rho_y^{(j)} = \frac{1}{2} \left(I + \cos \phi_y^{(j)} X + \sin \phi_y^{(j)} Y \right),$$

for some angle $\phi_y^{(j)} \in \mathbb{R}$ and with no Z -component.

This equatorial-state assumption is satisfied by common QML encoders where data are mapped into phases and superpositions via single-qubit rotations and Hadamard-type preparation such as circuits of the form $H \rightarrow R_Z(\phi_y^{(j)})$ on each qubit (Schuld & Killoran, 2019; Pérez-Salinas et al., 2020; Hatakeyama-Sato et al., 2023). Beyond QML, equatorial states also play a central role in quantum communication and quantum key distribution (QKD), where they are used for phase encoding and coherence-based information transfer (Fisher et al., 2014; Xiao et al., 2014). Thus, analyzing privacy amplification of GD channel under this assumption is both realistic and practically meaningful.

We consider the n -qubit GD channel acting independently on every qubit as follow:

$$f_{\text{GD}}^{(\eta)} = \bigotimes_{j=1}^n A_{\text{GD}}^{(\eta)},$$

We now establish a contraction bound for $f_{\text{GD}}^{(\eta)}$ under Assumption 4.8 in Lemma B.11.

Lemma B.11. *Let $f_{\text{GD}}^{(\eta)}$ be the n -qubit GD channel defined above, and assume the encoder f_{enc} satisfies Assumption 4.8. Then the trace-distance contraction coefficient of $f_{\text{GD}}^{(\eta)}$ over the encoder family $\{\rho_y\}_{y \in \mathbb{Y}}$ satisfies*

$$\kappa(f_{\text{GD}}^{(\eta)}) := \sup_{y \neq y'} \frac{D_1(f_{\text{GD}}^{(\eta)}(\rho_y) \| f_{\text{GD}}^{(\eta)}(\rho_{y'}))}{D_1(\rho_y \| \rho_{y'})} \leq |1 - 2\eta|.$$

Proof. For each y , we have

$$\rho_y = \bigotimes_{j=1}^n \rho_y^{(j)}, \quad \rho_y^{(j)} = \frac{1}{2} \left(I + \cos \phi_y^{(j)} X + \sin \phi_y^{(j)} Y \right).$$

Let $\Delta = \rho_y - \rho_{y'}$ for two distinct inputs $y \neq y'$. Expanding Δ in the n -qubit Pauli basis, we have:

$$\Delta = \sum_{P \in \mathcal{P}_n} c_P P,$$

where $\mathcal{P}_n = \{I, X, Y, Z\}^{\otimes n}$ is the n -qubit Pauli group, and $c_P \in \mathbb{R}$ since Δ is Hermitian.

Because each single-qubit factor $\rho_y^{(j)}$ contains only I , X , and Y components and no Z component, any product state $\rho_y = \bigotimes_j \rho_y^{(j)}$ expands only in Pauli strings whose single-qubit factors are in $\{I, X, Y\}$. The same holds for $\rho_{y'}$, and therefore their difference $\Delta = \rho_y - \rho_{y'}$ has no support on any string consisting solely of I 's and Z 's. In particular,

$$c_P = 0 \quad \text{for all } P \in \mathcal{P}_n \text{ such that } P \in \{I, Z\}^{\otimes n}.$$

Equivalently, every nonzero coefficient c_P corresponds to a Pauli string P that contains at least one factor X or Y .

The n -qubit GD channel acts diagonally in the Pauli basis:

$$f_{\text{GD}}^{(\eta)}(P) = \lambda_P P,$$

where

$$\lambda_P = \prod_{j=1}^n \lambda_{P_j}, \quad \lambda_I = \lambda_Z = 1, \quad \lambda_X = \lambda_Y = 1 - 2\eta,$$

and $P = P_1 \otimes \cdots \otimes P_n$ with $P_j \in \{I, X, Y, Z\}$. Thus, for any Pauli string P that contains at least one X or Y , we have

$$\lambda_P = (1 - 2\eta)^k$$

for $k \geq 1$. As a result, we have:

$$|\lambda_P| \leq |1 - 2\eta|.$$

It implies that:

$$f_{\text{GD}}^{(\eta)}(\Delta) = \sum_{P \in \mathcal{P}_n} c_P \lambda_P P,$$

with each nonzero coefficient satisfying $|\lambda_P| \leq |1 - 2\eta|$. As a linear map on the subspace spanned by Pauli strings with at least one X or Y , $f_{\text{GD}}^{(\eta)}$ is diagonal in an orthonormal operator basis with eigenvalues bounded in modulus by $|1 - 2\eta|$. Thus, its operator norm on any unitarily invariant norm, in particular the trace norm, is at most $|1 - 2\eta|$ on this subspace. Concretely,

$$\|f_{\text{GD}}^{(\eta)}(\Delta)\|_1 \leq |1 - 2\eta| \|\Delta\|_1.$$

Since $D_1(\rho\|\sigma) = \frac{1}{2}\|\rho - \sigma\|_1$, we conclude that for all $y \neq y'$,

$$\frac{D_1(f_{\text{GD}}^{(\eta)}(\rho_y) \| f_{\text{GD}}^{(\eta)}(\rho_{y'}))}{D_1(\rho_y\|\rho_{y'})} = \frac{\frac{1}{2}\|f_{\text{GD}}^{(\eta)}(\Delta)\|_1}{\frac{1}{2}\|\Delta\|_1} \leq |1 - 2\eta|.$$

Taking the supremum over all $y \neq y'$ gives the desired bound. \square

Finally, similar to the amplification analysis for depolarizing noise and GAD noise, we now derive a privacy amplification theorem for the GD channel acting on all qubits. The result follows immediately by combining the contraction bound in Lemma B.11 with the classical post-processing and distribution-decomposition tools used earlier.

Theorem 4.9. *Let $A : \mathbb{X} \rightarrow \mathcal{P}(\mathbb{Y})$ be a classical mechanism satisfying (ε, δ) -DP, and let*

$$Q^{(\eta)} := f_{\text{mea}} \circ f_{\text{GD}}^{(\eta)} \circ f_{\text{enc}}$$

be an n -qubit quantum mechanism where $f_{\text{GD}}^{(\eta)}$ is the n -qubit GD channel defined above and f_{enc} satisfies Assumption 4.8. Then the composed mechanism $Q^{(\eta)} \circ A$ satisfies (ε', δ') -DP with

$$\varepsilon' = \varepsilon, \quad \delta' = |1 - 2\eta| \cdot \delta.$$

Proof. Let $\mu = A(x)$ and $\nu = A(x')$ be the output distributions of A on neighboring inputs x, x' . As in Theorem 4.7, we apply Lemma B.1 to decompose μ, ν with parameter $\theta = D_{e^\varepsilon}(\mu\|\nu) \leq \delta$ and reduce the analysis to the worst-case pair of orthogonal inputs. Using Lemma B.2 and Lemma B.3, we can bound

$$D_{e^\varepsilon}(\mu Q^{(\eta)} \| \nu Q^{(\eta)}) \leq \theta \cdot \sup_{\rho \neq \rho'} D_1(f_{\text{GD}}^{(\eta)}(\rho) \| f_{\text{GD}}^{(\eta)}(\rho')),$$

where the supremum is taken over encoded states ρ, ρ' in the image of f_{enc} .

By Lemma B.11,

$$D_1(f_{\text{GD}}^{(\eta)}(\rho) \| f_{\text{GD}}^{(\eta)}(\rho')) \leq |1 - 2\eta| D_1(\rho\|\rho') \leq |1 - 2\eta|.$$

Therefore,

$$D_{e^\varepsilon}(\mu Q^{(\eta)} \| \nu Q^{(\eta)}) \leq \theta |1 - 2\eta| \leq |1 - 2\eta| \delta,$$

which yields the claimed privacy parameters $\varepsilon' = \varepsilon$ and $\delta' = |1 - 2\eta| \delta$. \square

Table 1. Dataset descriptions.

Dataset	Image Dims.	Training	Testing	No. of Labels	Description
MNIST	28×28	60,000	10,000	10	Handwritten digits
USPS	16×16	$\approx 7,300$	$\approx 2,000$	10	Scanned U.S. postal envelopes
FashionMNIST	28×28	60,000	10,000	10	Clothing items
CIFAR-10	$32 \times 32 \times 3$	50,000	10,000	10	Natural objects items

C. Implementation

We implement all experiments with Python 3.8. Each experiment is conducted on a single GPU-assisted compute node installed with a Linux 64-bit operating system. Our testbed resources include 72 CPU cores with 377 GB of RAM in total. Our allocated node is also provisioned with 2 GPUs with 40GB of VRAM per GPU.

Implementation of HYPER-Q. HYPER-Q was implemented using the PennyLane QML simulator (Bergholm et al., 2022). The detailed architecture implements the general mechanism proposed and analyzed in Section 4. Specifically, each input image first passes through two convolutional layers, each followed by batch normalization and max pooling to reduce spatial dimensions and extract salient features. The resulting feature maps are flattened and passed through two fully connected layers to produce a low-dimensional feature vector. This vector is then encoded into a quantum circuit (with 5-10 qubits) comprising three alternating layers of single-qubit rotations (implemented via RX gates) and entangling layers. This corresponds to the encoding function f_{enc} , where Hermitian generators are given by RX gates. The entangling layers employ a circular arrangement of CNOT gates, such that each qubit i is entangled with qubit $i + 1$, with the last qubit entangled with the first. A projective measurement is applied in the computational basis to extract the quantum outputs, which are then processed by a final fully connected layer to produce the prediction.

Additionally, the classical and quantum noise levels are set as follows. Given a target differential privacy budget (ε', δ') , we first fix the quantum depolarizing noise factor η , and then calibrate the classical Gaussian noise variance σ^2 to satisfy the budget based on Theorem 4.1. Specifically, σ^2 is chosen so that the classical mechanism A achieves (ε, δ) -DP with

$$\varepsilon = \varepsilon', \quad \delta = \frac{\delta' - \frac{\eta(1-e^\varepsilon)}{d}}{1 - \eta}.$$

The variance σ^2 is then computed using the Analytic Gaussian mechanism (Balle & Wang, 2018), ensuring that the classical mechanism A satisfies (ε, δ) -DP and the composed mechanism $Q^{(\eta)} \circ A$ satisfies the target (ε', δ') -DP.

Justification for QML architecture. The selection of the QML architecture for our experimental evaluation is consistent with established practices in the QML and quantum differential privacy literature, where models on the scale of 2 to 12 qubits are standard due to the computational limits of simulators and current hardware (Havlíček et al., 2019; Du et al., 2021a; Hur et al., 2022; Melo et al., 2023; Watkins et al., 2023; Long et al., 2025). Our objective in this study is to analyze the performance and stability of the HYPER-Q DP mechanism within a hybrid QML model rather than to optimize the underlying QML model for state-of-the-art classification accuracy. While large-scale noisy quantum training remains an open challenge characterized by barren plateaus and circuit depth constraints, we demonstrate that our HYPER-Q effectively scales and remains stable as the number of qubits increases by experimental results in Section F.4 and Section F.6.

D. Description of Datasets & Baselines

Datasets: We evaluate our approach on three image classification datasets: MNIST (Lecun et al., 1998), FashionMNIST (Xiao et al., 2017), and USPS (Hull, 2002). Table 1 briefly describes each of them.

Classical DP Mechanisms: In order to evaluate our DP mechanism HYPER-Q, we compare it against classical DP mechanisms. Below, we summarize DP mechanisms used for our comparison:

- **Basic Gaussian.** The Gaussian mechanism is a standard approach for providing (ε, δ) -DP. The Gaussian mechanism introduces noise from a normal distribution with zero mean and a variance calibrated to predefined privacy parameters (Dong et al., 2022). It's well-suited for functions whose sensitivity is measured using the ℓ_2 norm. Given a function f with a construction bound L_{cons} measured in ℓ_2 norm, the mechanism achieves (ε, δ) -DP by adding noise $\mathcal{N}(0, \sigma^2 I)$

with σ is computed as:

$$\sigma = \sqrt{2 \ln\left(\frac{1.25}{\delta}\right) L_{\text{cons}}/\varepsilon}$$

- **Analytic Gaussian.** The analytic Gaussian mechanism improves on the basic Gaussian approach by exploiting tighter bounds derived from the privacy loss distribution (Balle & Wang, 2018). Specifically, we can implicitly characterize the privacy loss as (Cullen et al., 2024):

$$\delta(\varepsilon) = \Phi\left(-\frac{L_{\text{cons}}}{2\sigma} + \frac{\varepsilon\sigma}{L_{\text{cons}}}\right) - e^\varepsilon \cdot \Phi\left(-\frac{L_{\text{cons}}}{2\sigma} - \frac{\varepsilon\sigma}{L_{\text{cons}}}\right)$$

where $\Phi(\cdot)$ is the cumulative distribution function of the standard Gaussian distribution. This formulation allows us to numerically solve for the minimum σ required to satisfy a target (ε, δ) .

- **DP-SGD.** The Differentially Private Stochastic Gradient Descent (DP-SGD) algorithm achieves privacy by clipping per-sample gradients and adding calibrated Gaussian noise during each optimization step (Abadi et al., 2016). As a gradient-perturbation mechanism, DP-SGD is designed to provide (ε, δ) -DP while maintaining compatibility with large-scale deep learning. The privacy guarantee arises from controlling the sensitivity of gradient updates and injecting noise proportional to this sensitivity. Although DP-SGD is a well-established baseline in classical machine learning, its behavior in QML settings remains largely unexplored. Beyond a direct application presented in (Watkins et al., 2023), the interplay between DP-SGD’s gradient noise and quantum gradient estimation has not been systematically examined. For completeness, we include DP-SGD in our comparison as a representative gradient-level classical mechanism.

Classical ML Models: In order to evaluate the practical viability, we compare QML models armed with HYPER-Q with three classical ML models armed with classical DP mechanisms: Multi-Layer Perceptron (MLP), ResNet-9, and Vision Transformer (ViT). We describe the implementations of those classical ML models below:

- **MLP:** We implement an MLP with a feedforward network composed of fully connected layers and ReLU activations. It consists of one hidden layer with 100 units and a final linear output layer corresponding to the number of classes. It is identical to the default MLP from the Sci-Kit Learn library¹. We implemented it without the library as it is not tailored for GPU usage out of the box. Our *from scratch* version is parallelizable on GPUs.
- **ResNet-9:** We implement a ResNet-9 model inspired by the original in (He et al., 2016). It is comprised of a series of convolutional layers and two residual blocks that include skip connections. It processes inputs through increasing feature dimensions: [32, 64, 128]. We employ batch normalization and ReLU activations throughout the model following by MaxPooling layers. The model ends with a fully-connected layer for classification.
- **ViT:** We implement a ViT model inspired by (Dosovitskiy et al., 2021). It splits input images into non-overlapping patches and linearly embeds them before adding positional encodings and a class token. Multiple self-attention layers processes each sequence before classifying via a fully connected head applied to the class token.

E. Adversarial Training and Testing

We evaluate the adversarial robustness of HYPER-Q via an adversarial training and testing framework inspired by the PixelDP mechanism (Lecuyer et al., 2019). Similar to PixelDP, during training, we define a *construction attack bound* L_{cons} to represent the theoretical robustness guarantee in terms of ℓ_2 norm. Specifically, this bound establishes the maximum allowable adversarial perturbation under which the model is certified to preserve its prediction capabilities. In our experiments, we vary this value where $L_{\text{cons}} = \{0.1, 0.2, 0.3, 0.4\}$. In both HYPER-Q and classical baseline models, ℓ_2 -based noise is injected directly into the input. This setup permits a fair comparison of robustness guarantees between quantum and classical models despite their underlying architectural differences.

¹<https://scikit-learn.org/stable/>

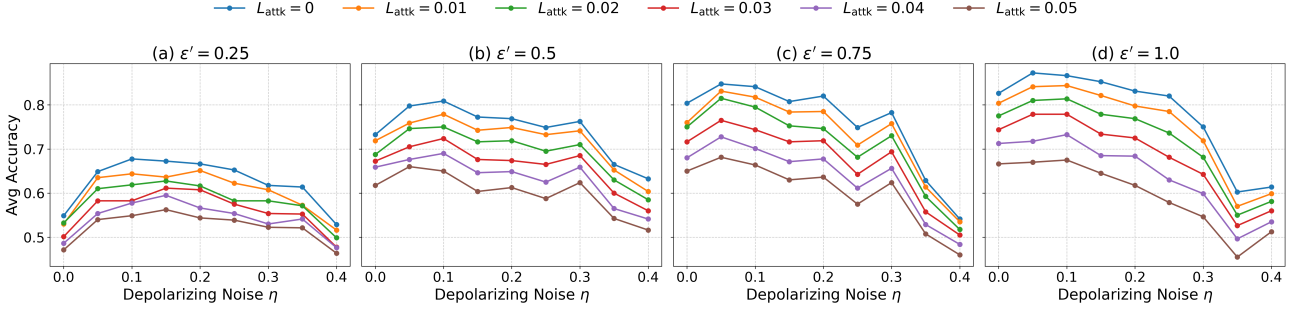


Figure 4. Impact of depolarizing noise η on model utility for the MNIST dataset. Subplots (a)-(d) show performance under varying privacy budgets $\varepsilon' \in \{0.25, 0.5, 0.75, 1.0\}$. Each curve represents the average accuracy against FGSM attacks with varying strengths $L_{\text{attk}} \in \{0, \dots, 0.05\}$.

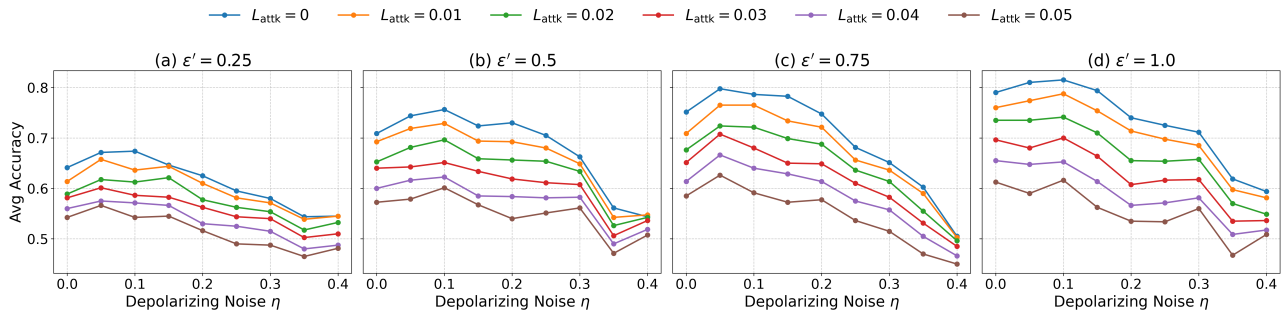


Figure 5. Impact of depolarizing noise η on model utility for the Fashion-MNIST dataset. Subplots (a)-(d) show performance under varying privacy budgets $\varepsilon' \in \{0.25, 0.5, 0.75, 1.0\}$. Each curve represents the average accuracy against FGSM attacks with varying strengths $L_{\text{attk}} \in \{0, \dots, 0.05\}$.

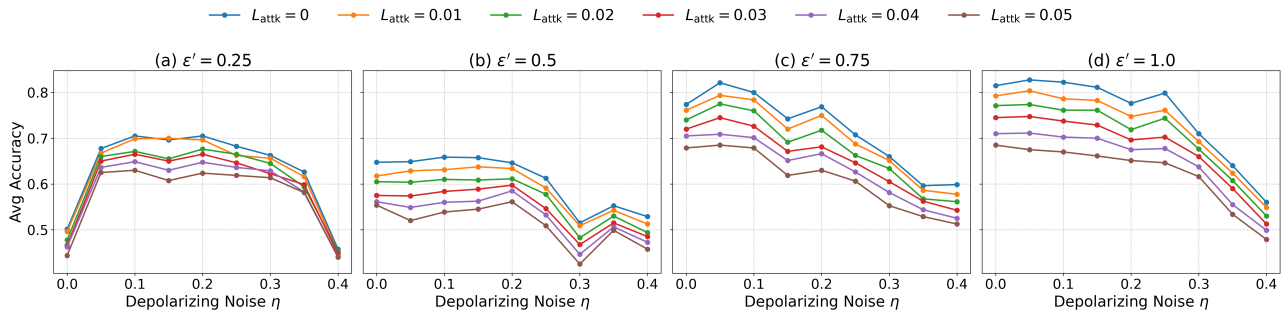


Figure 6. Impact of depolarizing noise η on model utility for the USPS dataset. Subplots (a)-(d) show performance under varying privacy budgets $\varepsilon' \in \{0.25, 0.5, 0.75, 1.0\}$. Each curve represents the average accuracy against FGSM attacks with varying strengths $L_{\text{attk}} \in \{0, \dots, 0.05\}$.

To evaluate empirical robustness beyond certified guarantees, we assess each model against adversarial perturbations constrained by the ℓ_∞ norm. Specifically, for every L_{cons} value, we experiment against empirical attack bounds L_{attk} . In our experiments, we vary this value where $L_{\text{attk}} = \{0, 0.01, 0.02, 0.03, 0.04, 0.05\}$ while implementing two adversarial attacks: Fast Gradient Sign Method (FGSM) and Projected Gradient Descent (PGD). With this, we are able to observe model performance under realistic threats that may not satisfy the constraints of our certified threat model. In addition, we adopt the randomized smoothing technique proposed by (Cohen et al., 2019) to provide certified predictions against adversarial examples.

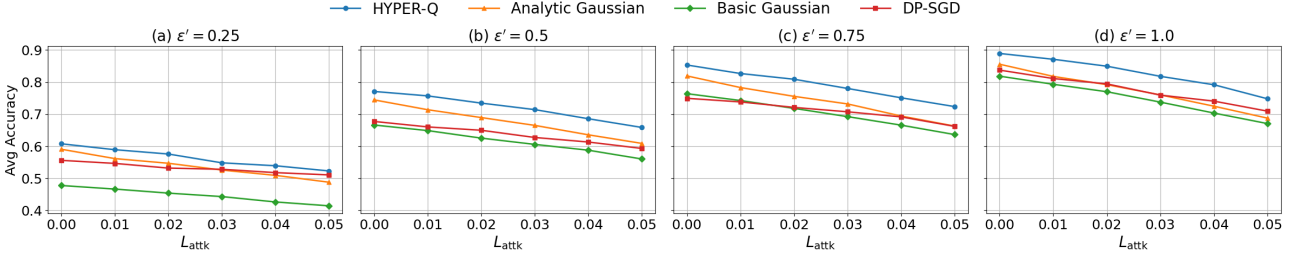


Figure 7. Accuracy of various noise-added mechanisms under the FGSM attack on the MNIST dataset with different ϵ' values and $\delta' = 1 \times 10^{-5}$. For each pair of $(L_{\text{attk}}, \epsilon')$, the reported accuracy is averaged over all L_{cons} settings. HYPER-Q is examined with $\eta = 0.1$.

F. Additional Experiments

F.1. Sensitivity Analysis of η (extended)

In this section, we present more details for sensitivity analysis in Section 5.1. Figures 4,5 and 6 collectively show that the relationship between depolarizing noise η and model performance exhibits a remarkably consistent structure across all three datasets: MNIST, Fashion-MNIST and USPS. Despite differences in dataset complexity, the accuracy curves share the same unimodal shape. Specifically, performance initially increases as η moves away from 0, reach a peak and, then declines once the quantum distortion dominates. This pattern is visible in every privacy budget $\epsilon' \in \{0.25, 0.5, 0.75, 1\}$ and across all attack bounds L_{attk} .

When comparing the location of the performance peaks across datasets, we observe a highly aligned trend. Under stricter privacy budgets ($\epsilon' \leq 0.5$), the best performance is usually achieved at $\eta = 0.1$ or $\eta = 0.05$. For example, MNIST and Fashion-MNIST peak at $\eta = 0.1$ and USPS similarly peaks at $\eta = 0.1 - 0.15$ for $\epsilon' = 0.25$. As the privacy requirement becomes more relaxed ($\epsilon' \geq 0.75$), all three datasets shift their peaks toward smaller noise levels, typically $\eta = 0.05$. We observe that the optimal η consistently falls within the narrow interval 0.05-0.15. Although η is often difficult to calibrate precisely in practice (Hu et al., 2023), this stable peak range provides a robust guideline that users can reliably calibrate η within this interval without requiring an exhaustive sweep.

F.2. Robustness Analysis of HYPER-Q (extended)

As in Section 5.2, we evaluate the adversarial robustness of HYPER-Q under the depolarizing noise level $\eta = 0.1$. We compare its performance with Basic Gaussian, Analytic Gaussian and DP-SGD mechanisms, ensuring that all methods are evaluated under the same privacy budget and applied to the same QML model. Figures 7, 8 and 9 present the results of the FGSM attack on the FashionMNIST and USPS datasets, respectively with $\epsilon' \in \{0.25, 0.5, 0.75, 1\}$. On MNIST and FashionMNIST, HYPER-Q consistently outperforms all baseline mechanisms across the evaluated privacy budgets. In contrast, on USPS, Analytic Gaussian achieves the highest accuracy for larger privacy budgets ($\epsilon' > 0.25$), while HYPER-Q yields the best performance under the strictest privacy constraint ($\epsilon' = 0.25$).

Figures 10, 11, and 12 report the performance under PGD attacks for HYPER-Q and the baseline mechanisms on MNIST, FashionMNIST, and USPS, respectively. The observed trends closely mirror those under FGSM attacks. Specifically, HYPER-Q consistently achieves the highest accuracy on MNIST and FashionMNIST, whereas Analytic Gaussian attains the best performance on USPS.

F.3. Comparative Benchmark with Classical Models

The HYPER-Q mechanism is intrinsically designed for QML models. This raises a critical question of practical viability: *Can a QML model protected by HYPER-Q compare to or outperform classical models that are protected by their own conventional privacy mechanisms?*. We illustrate the performance comparison of a QML model protected by HYPER-Q (with its empirically optimal quantum noise setting, $\eta = 0.1$) against three classical baselines: ResNet-9, ViT, and MLP, each protected by Analytic Gaussian noise. Figures 13, 14 and 15 illustrate the performance comparison between all models on MNIST, FashionMNIST and USPS datasets, respectively, while under the FGSM attack. In Figure 14, we observe that the ResNet-9 model, across all values of ϵ' , outperforms HYPER-Q and the other baseline models. However, it is noted that HYPER-Q is very comparable to the ResNet-9 model with larger values of ϵ' . Only at higher values of L_{attk} do we

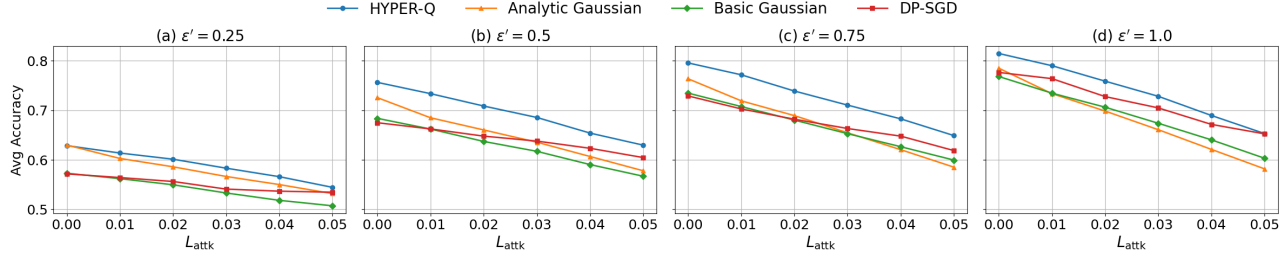


Figure 8. Accuracy of various noise-added mechanisms under the FGSM attack on the FashionMNIST dataset with different ϵ' values and $\delta' = 1 \times 10^{-5}$. For each pair of $(L_{\text{attk}}, \epsilon')$, the reported accuracy is averaged over all L_{cons} settings. HYPER-Q is examined with $\eta = 0.1$.

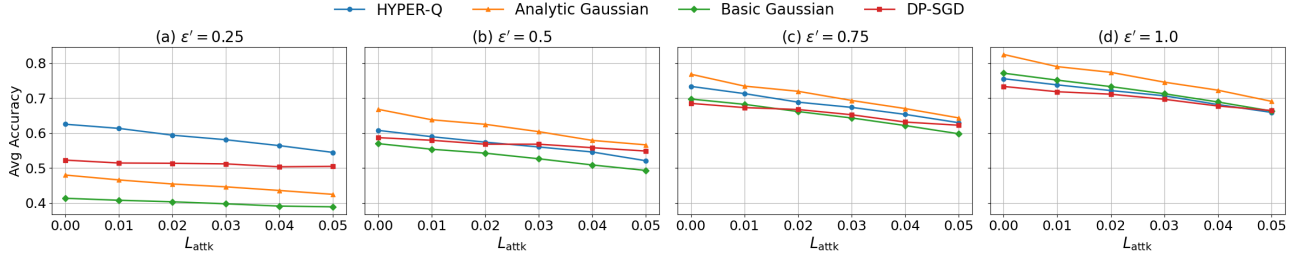


Figure 9. Accuracy of various noise-added mechanisms under the FGSM attack on the USPS dataset with different ϵ' values and $\delta' = 1 \times 10^{-5}$. For each pair of $(L_{\text{attk}}, \epsilon')$, the reported accuracy is averaged over all L_{cons} settings. HYPER-Q is examined with $\eta = 0.1$.

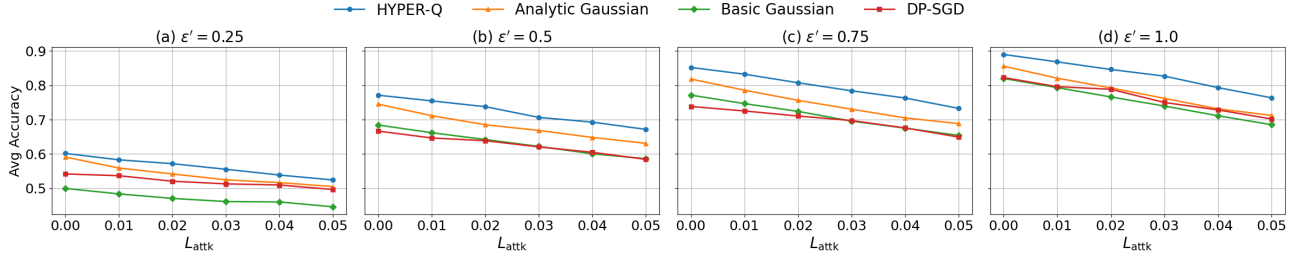


Figure 10. Accuracy of various noise-added mechanisms under the PGD attack on the MNIST dataset with different ϵ' values and $\delta' = 1 \times 10^{-5}$. For each pair of $(L_{\text{attk}}, \epsilon')$, the reported accuracy is averaged over all L_{cons} settings. HYPER-Q is examined with $\eta = 0.1$.

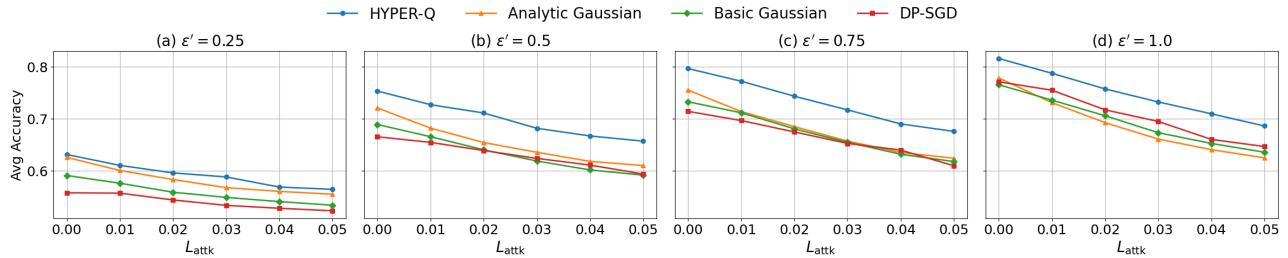


Figure 11. Accuracy of various noise-added mechanisms under the PGD attack on the FashionMNIST dataset with different ϵ' values and $\delta' = 1 \times 10^{-5}$. For each pair of $(L_{\text{attk}}, \epsilon')$, the reported accuracy is averaged over all L_{cons} settings. HYPER-Q is examined with $\eta = 0.1$.

observe noticeable separation between the two models. Contrarily, for the USPS dataset, HYPER-Q dominates all other baseline models when $\epsilon' \in \{0.25, 0.5\}$. Specifically, compared to the ResNet-9 model, HYPER-Q maintains an $\approx 30\%$ higher average accuracy when $\epsilon' = 0.25$. This value drops to $\approx 2\%$ when $\epsilon' = 0.5$. The ResNet-9 model becomes more competitive as $\epsilon' \in \{0.75, 1.0\}$, where it is comparable to HYPER-Q and then outperforms it by $\approx 5\%$, respectively. An interesting observation is the subtle fluctuations of the MLP and quick degradation across all values of ϵ' . HYPER-Q and the other baselines are much more stable across all values. The results shown in Figures 16, 17, and 18 illustrate the comparative

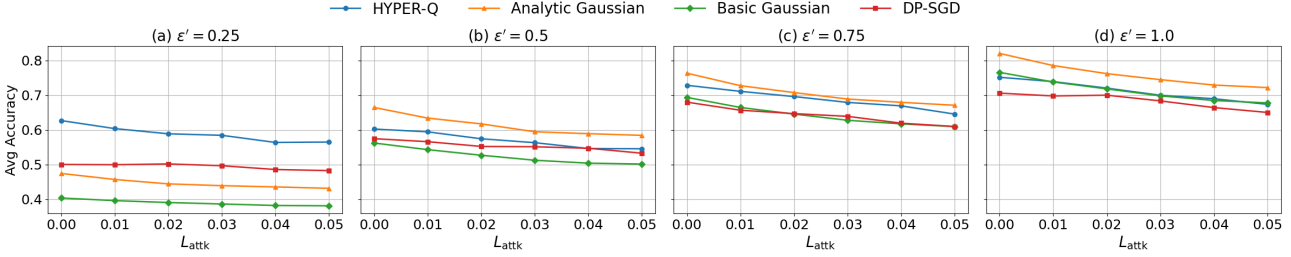


Figure 12. Accuracy of various noise-added mechanisms under the PGD attack on the USPS dataset with different ϵ' values and $\delta' = 1 \times 10^{-5}$. For each pair of $(L_{\text{attk}}, \epsilon')$, the reported accuracy is averaged over all L_{cons} settings. HYPER-Q is examined with $\eta = 0.1$.

performance of HYPER-Q and our baseline models when subjected to the PGD attack and are virtually identical in nature to the results of the FGSM attack on all three datasets.

F.4. Empirical Analysis of Dimensional Scalability

To address the practical scalability of HYPER-Q, we empirically investigated the impact of the Hilbert space dimension $d = 2^n$ on the reduction of the required classical noise. While Theorem 1 introduces an additive term $\frac{\eta(1-e^\epsilon)}{d}$ that ostensibly shrinks as the system scales, our analysis reveals that the privacy amplification stabilizes rather than vanishes.

Figure 19 presents the average percentage reduction in classical noise variance (σ^2) as a function of the number of qubits n , ranging from 1 to 29, across various quantum noise levels $\eta \in [0.05, 0.4]$. The results highlight two observations. For small-scale systems, we observe a massive reduction in the required classical noise, exceeding 90% for $n < 3$. In this regime, the dimension-dependent term $\frac{1}{d}$ in Theorem 1 is dominant, providing a significant bonus to the privacy budget. On the other hand, as the number of qubits increases and the $1/d$ term vanishes, the noise reduction does not drop to zero. Instead, the curves flatten into a stable, non-zero level. This represents the scale-independent multiplicative amplification $(1 - \eta)$ derived in our theoretical framework. For instance, with $\eta = 0.4$, the mechanism maintains a consistent noise reduction of approximately 8% even at $n = 29$ (where $d \approx 5 \times 10^8$).

F.5. Empirical Verification of Utility Bound Tightness

To rigorously assess the tightness of the theoretical utility bound derived in Theorem 3, we conducted an empirical analysis comparing the observed worst-case error against the bound. Theorem 3 characterizes the stability of the mechanism by bounding the maximum deviation $\text{Error} = \sup_x |\mathcal{M}_{\text{full}}(x) - \mathcal{M}_{\text{clean}}(x)|$. The bound states that

$$\Pr \left(\text{Error} \leq L_\infty \cdot \sigma \sqrt{2 \ln \frac{2d_X}{p} + 2\eta \|E_{\text{exp}}\|_{\text{op}}} \right) \geq 1 - p$$

where $L_\infty = 2(1 - \eta) \|E_{\text{exp}}\|_{\text{op}} \|W\|_\infty (\sum_j \|H_j\|_{\text{op}})$.

We evaluated the tightness of our bound by measuring the ratio between the maximum empirical error observed in simulation and the theoretical bound $\text{Bound}(\sigma, \eta, p) = L_\infty \sigma \sqrt{2 \ln(2d_X/p) + 2\eta \|E_{\text{exp}}\|_{\text{op}}}$. In particular, given a sample set S , the ratio is calculated by:

$$\text{Ratio} = \frac{\max_{x \in S} |\mathcal{M}_{\text{full}}(x) - \mathcal{M}_{\text{clean}}(x)|}{\text{Bound}(\sigma, \eta, p)}$$

In this experiment, we set the failure probability to $p = 0.01$. That ensures the theoretical bound holds with a 99% confidence level. We computed the Ratio for each (σ, η) configuration using a sample size of $|S| = 10000$, where a value approaching 1 indicates a tight bound. Figure 20 presents the resulting ratios across the parameter grid. We observe that in low-noise settings, such as $(\sigma, \eta) = (0.5, 0)$, the ratio reaches significant magnitudes (e.g., 0.923), confirming that the bound effectively captures the worst-case error. While the bound becomes looser as the total noise magnitude increases, it remains non-trivial. Notably, in the absence of classical noise ($\sigma = 0$), the ratios remain constant across all η . This behavior is attributed to the linearity of the depolarizing channel, where both the empirical error and the theoretical quantum term $(2\eta \|E_{\text{exp}}\|_{\text{op}})$ scale linearly with η .

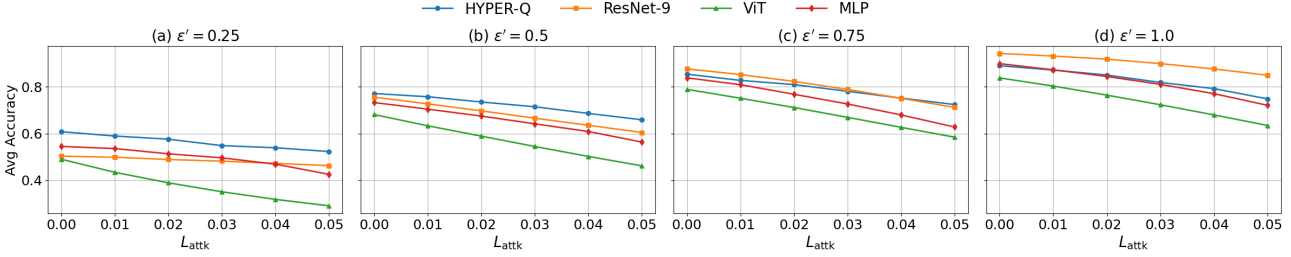


Figure 13. Accuracy comparison between the QML model protected by HYPER-Q and three classical baselines (ResNet-9, ViT, and MLP) protected by Analytic Gaussian noise under the FGSM attack on the MNIST dataset. The HYPER-Q model is evaluated with its empirically best quantum noise setting ($\eta = 0.1$). For each $(L_{\text{attk}}, \epsilon')$ pair, the reported accuracy is averaged over all L_{cons} settings. $\delta' = 1 \times 10^{-5}$ for all settings.

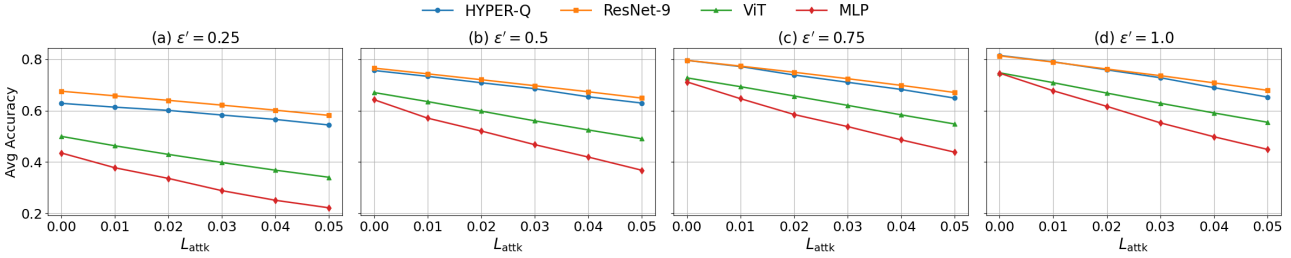


Figure 14. Accuracy comparison between the QML model protected by HYPER-Q and three classical baselines (ResNet-9, ViT, and MLP) protected by Analytic Gaussian noise under the FGSM attack on the FashionMNIST dataset. The HYPER-Q model is evaluated with its empirically best quantum noise setting ($\eta = 0.1$). For each $(L_{\text{attk}}, \epsilon')$ pair, the reported accuracy is averaged over all L_{cons} settings. $\delta' = 1 \times 10^{-5}$ for all settings.

F.6. Performance Analysis on CIFAR-10

To evaluate the robustness of HYPER-Q on more complex data, we extend our experiments to CIFAR-10, a significantly more challenging benchmark than MNIST and USPS. Unlike grayscale datasets, CIFAR-10 consists of RGB images with higher variability and richer feature structure, requiring a larger quantum feature map. For this setting, we employ a 10-qubit variational QML model and compare HYPER-Q with three classical baselines under a fixed privacy budget $\epsilon' = 1$.

Figure 21 shows the test accuracy as a function of attack strength $L_{\text{attk}} \in \{0, 0.01, \dots, 0.05\}$. Across all models, accuracy decreases as the attack strength increases, but the rate of degradation varies significantly. HYPER-Q begins at 73.9% accuracy at $L_{\text{attk}} = 0$ and declines smoothly to 47.7% at $L_{\text{attk}} = 0.05$. This degradation profile is comparable to ResNet-9, which starts at a higher baseline of 86.0% but similarly drops to 48.7% at the highest attack bound. In contrast, ViT and MLP degrade much more rapidly, falling from 75.9% and 69.3% initially to only 14.2% and 10.8% at $L_{\text{attk}} = 0.05$, respectively.

These results highlight two insights. First, even for a high-dimensional image dataset requiring a deeper quantum representation, HYPER-Q remains competitive with classical baselines under moderate attack strengths. Second, while classical deep models exhibit higher clean accuracy, their robustness diminishes sharply under increasing perturbation, whereas HYPER-Q shows a more controlled and stable decline. This demonstrates that the hybrid-noise mechanism HYPER-Q continues to offer meaningful utility benefits in more complex, higher-qubit QML settings.

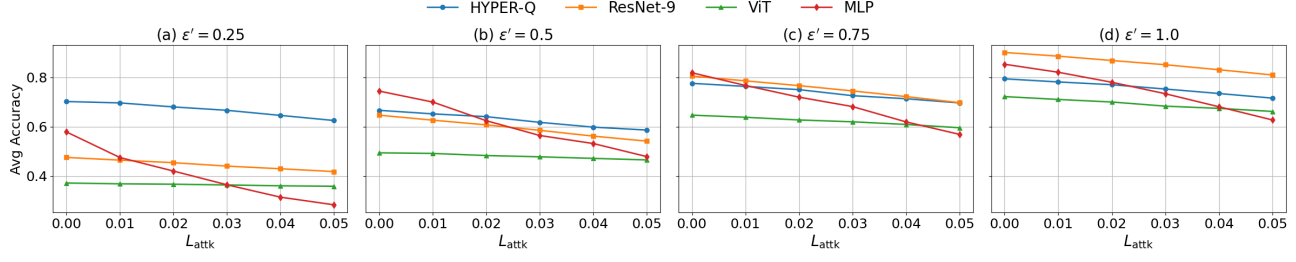


Figure 15. Accuracy comparison between the QML model protected by HYPER-Q and three classical baselines (ResNet-9, ViT, and MLP) protected by Analytic Gaussian noise under the FGSM attack on the USPS dataset. The HYPER-Q model is evaluated with its empirically best quantum noise setting ($\eta = 0.1$). For each $(L_{\text{attk}}, \epsilon')$ pair, the reported accuracy is averaged over all L_{cons} settings. $\delta' = 1 \times 10^{-5}$ for all settings.

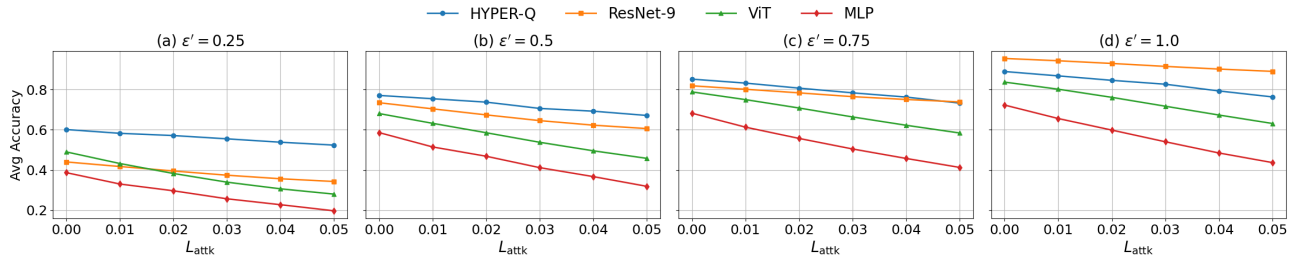


Figure 16. Accuracy comparison between the QML model protected by HYPER-Q and three classical baselines (ResNet-9, ViT, and MLP) protected by Analytic Gaussian noise under the PGD attack on the MNIST dataset. The HYPER-Q model is evaluated with its empirically best quantum noise setting ($\eta = 0.1$). For each $(L_{\text{attk}}, \epsilon')$ pair, the reported accuracy is averaged over all L_{cons} settings. $\delta' = 1 \times 10^{-5}$ for all settings.

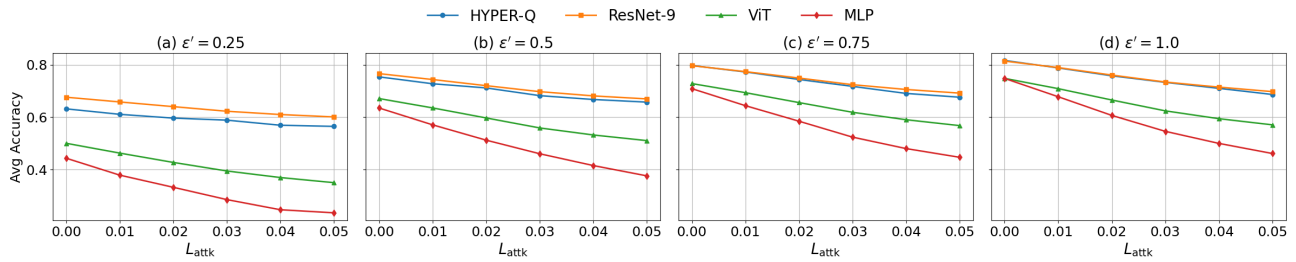


Figure 17. Accuracy comparison between the QML model protected by HYPER-Q and three classical baselines (ResNet-9, ViT, and MLP) protected by Analytic Gaussian noise under the PGD attack on the FashionMNIST dataset. The HYPER-Q model is evaluated with its empirically best quantum noise setting ($\eta = 0.1$). For each $(L_{\text{attk}}, \epsilon')$ pair, the reported accuracy is averaged over all L_{cons} settings. $\delta' = 1 \times 10^{-5}$ for all settings.

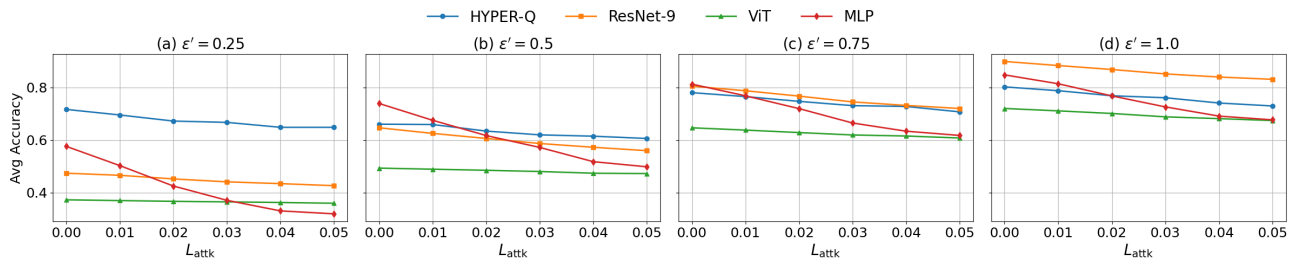


Figure 18. Accuracy comparison between the QML model protected by HYPER-Q and three classical baselines (ResNet-9, ViT, and MLP) protected by Analytic Gaussian noise under the PGD attack on the USPS dataset. The HYPER-Q model is evaluated with its empirically best quantum noise setting ($\eta = 0.1$). For each $(L_{\text{attk}}, \epsilon')$ pair, the reported accuracy is averaged over all L_{cons} settings. $\delta' = 1 \times 10^{-5}$ for all settings.

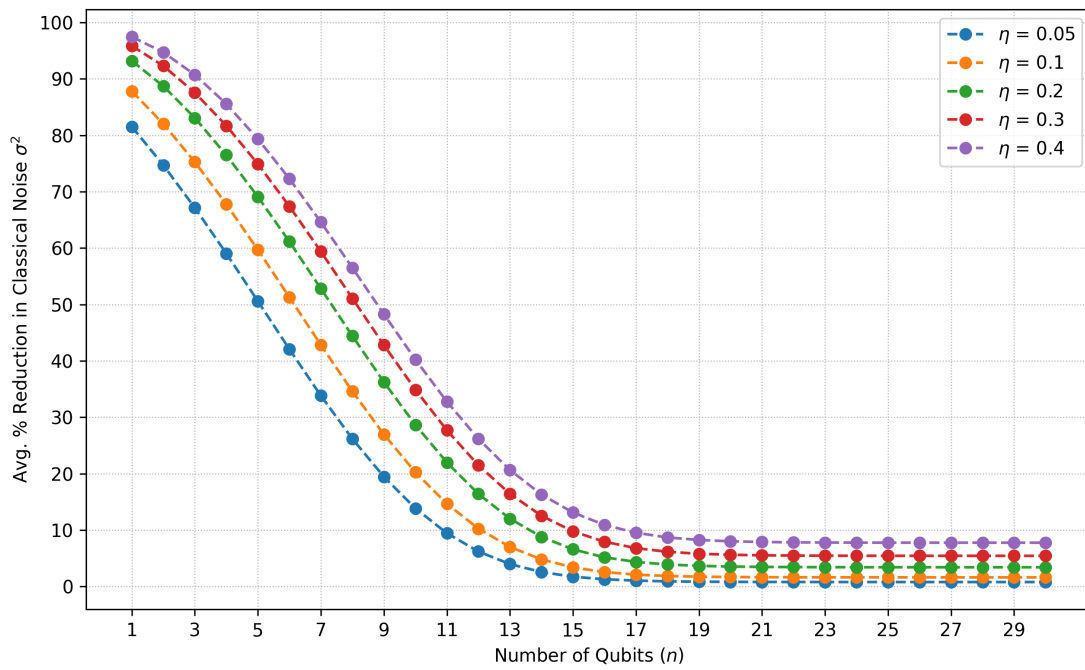


Figure 19. Effect of Quantum Noise Level on Classical-Noise Reduction Across Scaling Qubit Counts

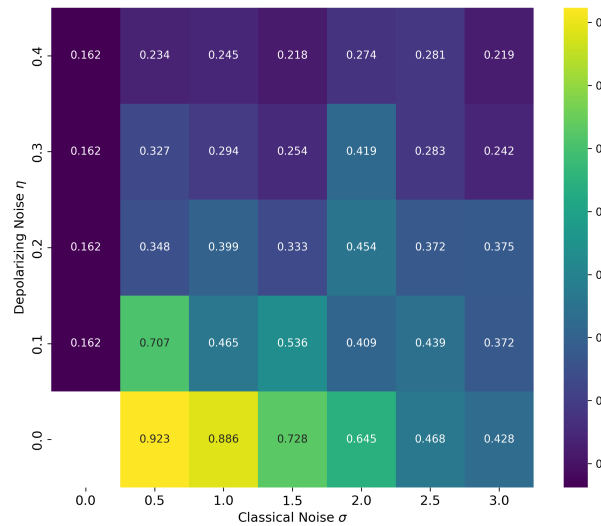


Figure 20. Heatmap of the ratio between the actual utility loss and the theoretical bound across (η, σ) values.

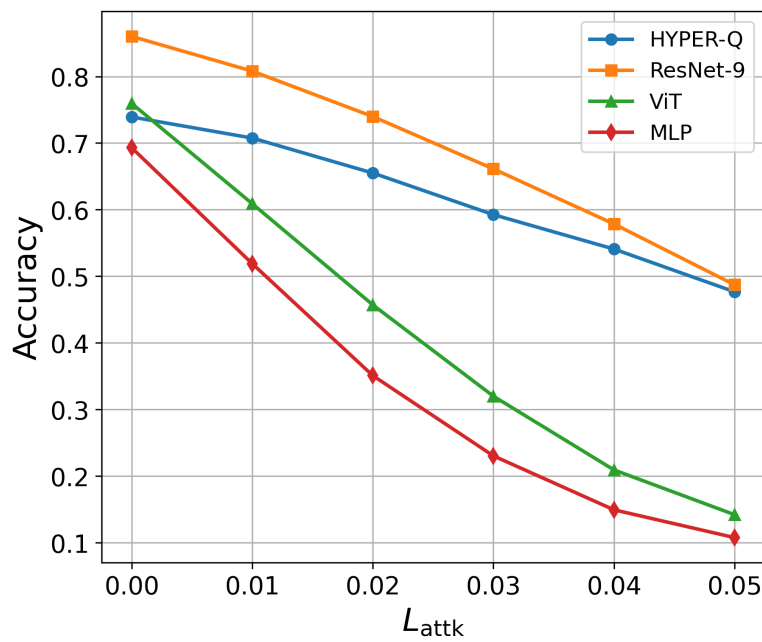


Figure 21. Performance of HYPER-Q and classical baselines (ResNet-9, ViT, and MLP) on CIFAR-10 under varying attack strengths L_{attk} with a fixed privacy budget $\varepsilon' = 1$.